Applied Food Research 6 (2026) 102325

Contents lists available at ScienceDirect

Applied Food Research

journal homepage: www.elsevier.com/locate/afres

Ethanolic extract from giant red shrimp (*Aristaeomorpha foliacea*) cephalothorax: A waste-derived sustainable ingredient with antioxidant and anti-lipotoxic activity

Ilaria Serra [a,b], Federica Mancarella [a], Paola Semeraro [a,1], Maria Tufariello [c], Alessandro Miraglia [d], Marcello Chieppa [d], Aurelia Scarano [c], Angelo Santino [c], Daniele Vergara [a], Elisa Bisconti [a], Francesco Vari [a], Ludovico Valli [a,e], Livia Giotta [a,e,*], Anna Maria Giudetti [a,*], Francesco Milano [c]

[a] Dipartimento di Scienze e Tecnologie Biologiche e Ambientali, Università del Salento, S.P. Lecce-Monteroni, I-73100 Lecce, Italy
[b] Dipartimento di Fisiologia e Farmacologia "V. Erspamer", Università degli Studi di Roma La Sapienza, P.le Aldo Moro 5, 00185, Rome, Italy
[c] Istituto di Scienze delle Produzioni Alimentari (ISPA), Consiglio Nazionale delle Ricerche (CNR), UOS Lecce, S.P. Lecce-Monteroni, I-73100 Lecce, Italy
[d] Dipartimento di Medicina Sperimentale, Università del Salento, S.P. Lecce-Monteroni, I-73100 Lecce, Italy
[e] Consorzio Interuniversitario Nazionale per la Scienza e Tecnologia dei Materiali (INSTM), Unità di Lecce, Lecce, Italy

ARTICLE INFO

Keywords:
Seafood industry waste
Xanthophylls
Polyphenolics
Oxidative stress
Hepatic cells
Intestinal cells

ABSTRACT

Shrimp by-products are a promising source of bioactives. This study investigated the composition and the bioactivity of a preparation obtained in mild conditions via ethanol extraction from the cephalothorax of the Mediterranean red shrimp species *Aristaeomorpha foliacea*. The crude extract (CE) exhibited high levels of astaxanthin (AST) and polyphenols, which contributed to its notable antioxidant activity. Monounsaturated fatty acids dominated the lipid profile of CE (46%), reflecting a typical trait of deep-sea species, while polyunsaturated and saturated fatty acids accounted for 33% and 21%, respectively. Chemical fractionation yielded a hydrophobic fraction (HF; AST-enriched) and a polar fraction (PF; polyphenols-enriched). In hepatic (HuH7) and intestinal (HCT15) human cells, CE induced dose-dependent lipid droplet accumulation and protected against palmitic acid-induced lipotoxicity: it restored cell viability, reduced reactive oxygen species, prevented lipid peroxidation and induced modulation of antioxidant enzymes, including catalase, glutathione peroxidase, and superoxide dismutase. While the HF alone partially reproduced these effects, full antioxidant and cytoprotective activity required the synergistic contribution of both fractions. These findings support the potential application of shrimp waste-derived ethanol extracts as sustainable sources of functional ingredients for oxidative stress-related conditions.

1. Introduction

Oxidative stress results from an imbalance between the production of reactive oxygen species (ROS) and body's antioxidant defences. Managing cellular oxidative stress is vital for preventing and treating numerous non-communicable diseases (NCDs), as it triggers chronic inflammation (Hussain et al., 2016; Seyedsadjadi & Grant, 2021). This interaction drives atherosclerosis (Donia & Khamis, 2021; Zhazykbayeva et al., 2020), aggravates liver disease progression (Li et al., 2016) and respiratory disease severity (Dua et al., 2019), and is central to inflammatory bowel diseases (Moura et al., 2015), cancer, diabetes, and metabolic syndrome (Battino et al., 2021; Peña-Oyarzun et al., 2018). Carotenoids, including their oxygenated forms known as xanthophylls, exhibit antioxidant, anti-inflammatory, and anti-apoptotic properties and play a significant role in the prevention and treatment of NCDs. These compounds influence intracellular signalling pathways by modulating gene expression and reducing the production of inflammatory cytokines and oxidative stress markers

* Corresponding authors.
E-mail addresses: livia.giotta@unisalento.it (L. Giotta), anna.giudetti@unisalento.it (A.M. Giudetti).
[1] Present address: Istituto di Scienze dell'Atmosfera e del Clima (ISAC), Consiglio Nazionale delle Ricerche (CNR), UOS Lecce, S.P. Lecce-Monteroni, I-73100 Lecce, Italy.

https://doi.org/10.1016/j.afres.2026.102325
Received 24 November 2025; Received in revised form 11 May 2026; Accepted 23 June 2026
Available online 24 June 2026

(Bohn, 2019; Kaulmann & Bohn, 2014; Zuluaga et al., 2017).

Marine sources offer a wide variety of xanthophyll pigments, including fucoxanthin, astaxanthin (AST), and lutein, that have demonstrated high potential in mitigating oxidative damage (Bungau et al., 2019; Gammone et al., 2015). Similarly, polyunsaturated fatty acids (PUFAs) from fish and seafood, particularly omega-3 fatty acids such as eicosapentaenoic acid (EPA) and docosahexaenoic acid (DHA), exhibit anti-inflammatory properties. They modulate membrane phospholipids, improve mitochondrial function, and enhance the activity of endogenous antioxidant enzymes, which collectively contribute to cardiovascular protection and reduced oxidative stress (Djuricic & Calder, 2021; Oppedisano et al., 2020).

Xanthophylls and PUFAs thus represent promising candidates for the prevention and treatment of NCDs, and their integration into dietary interventions may offer significant health benefits. Blends of these bioactive compounds appear particularly interesting based on the synergistic antioxidant effects of AST and PUFAs (Saw et al., 2013). However, further research is required to understand their dose-dependent effects and their mechanisms of action, which would support the optimization of their therapeutic application.

Shrimp shell waste, a by-product of the seafood industry, represents a valuable resource of bioactive compounds such as AST and PUFAs. AST is naturally abundant in shrimp tissues that are typically discarded, such as exoskeleton and cephalothorax, and can be efficiently recovered using various methods, including enzymatic processes and supercritical CO_2 extraction (Aneesh et al., 2023; Cheong et al., 2020; Sánchez-Camargo et al., 2011). These extraction methods not only enable high-yield recovery of AST, but also ensure the preservation of its natural state, making it suitable for nutritional and biomedical applications (Deng et al., 2020; Fotodimas et al., 2024). Further techniques, such as ultrasonic-assisted extraction (Sharayei et al., 2021) or the use of neoteric solvents (Mancarella et al., 2025), have been developed to enhance the efficiency and sustainability of the process. AST is typically recovered from shrimp waste as a component of a lipid fraction, the so-called shrimp oil, which contains high levels of omega-3 fatty acids, including EPA and DHA (Aneesh et al., 2023; Gómez-Estaca et al., 2017; Sánchez-Camargo et al., 2011).

The biorefinery approach to shrimp shell waste enables not only the extraction of AST and PUFAs but also the recovery of other bioactives and additional high-value compounds such as proteins and chitin, in line with the principles of the circular economy model (Aneesh et al., 2023; Deng et al., 2020). This valorisation strategy reduces environmental pollution while adding economic value to what is traditionally regarded as a low-value and problematic by-product (Deng et al., 2020; Fotodimas et al., 2024). The sustainable utilization of shrimp shell waste for recovering bioactive compounds addresses therefore environmental challenges and offers considerable health and economic benefits. This approach aligns with global sustainability goals and resource efficiency frameworks, highlighting the potential of shrimp shell waste as a valuable resource in the food and health industries, particularly due to the combined antioxidant properties of AST and the health-promoting effects of PUFAs (Fotodimas et al., 2024; Gómez-Estaca et al., 2017). AST concentrations in shrimp oil vary considerably depending on species, anatomical part, and extraction method. Typical values range from 0.1 to 1 mg/g of lipid extract (Kaya et al., 2025; Roy et al., 2020; Wang et al., 2021), although values as high as 7 mg/g have been reported (Gómez-Estaca et al., 2017).

This paper focused on an AST-rich extract obtained from a seafood industry by-product, specifically the cephalothorax of Mediterranean red shrimps *Aristaeomorpha foliacea* (Risso, 1827). This species has been recently identified as particularly capable of AST uptake and storage (Magalhães et al., 2010; Mancarella et al., 2025). An environmentally friendly and economically viable approach, using ethanol, a generally recognized as safe (GRAS) solvent, has been employed for the extraction of the oleaginous fraction from *A. foliacea* cephalothorax. Its chemical composition and functional properties have been assessed by spectrophotometric and chromatographic techniques, gaining information not only on AST and fatty acids content, but also on more polar compounds including polyphenols. Furthermore, the therapeutic value of the extract was assessed by evaluating its antioxidant and anti-inflammatory properties in two human cell lines: HuH7 hepatocarcinoma and HCT15 colorectal adenocarcinoma cells. These cell models were selected to represent the liver and intestinal epithelium, which are the primary sites of exposure following oral administration of the extract. Finally, fractionation of the crude ethanol extract using ethyl acetate partitioning enabled the evaluation of how hydrophobic and polar bioactive compounds distinctly influence cellular responses to oxidative stress.

Despite the growing body of research on shrimp waste valorisation, most studies have often employed solvents of limited sustainability and safety such as chloroform, methanol and n-hexane and have focused mainly on astaxanthin and PUFA components (Raju et al., 2021). Importantly, no study has yet simultaneously characterized the full chemical profile of an ethanol-based extract from *A. foliacea* cephalothorax and investigated the distinct and synergistic contributions of its hydrophobic and polar fractions to antioxidant and anti-lipotoxic activity in human cell models. The present work therefore addresses these gaps by integrating compositional profiling with cell-based functional evaluation, providing novel evidence for the applicative potential of this seafood by-product as a sustainable functional ingredient.

2. Materials and methods

2.1. Materials

Synthetic (all-*E*)-AST ((all-*E*)-AST, ≥97%) was purchased from ThermoFisher Scientific. Ethyl acetate (EtAc, ≥99.7%), ethanol (96%), methanol (≥99.8%), 2,2′-Azino-bis(3-ethylbenzothiazoline-6-sulfonic acid) (ABTS, >98%) and sodium hydroxide pellets were purchased from Sigma-Aldrich and used as received. Ultrapure Milli-Q water, purified by a Millipore Milli-Q system (resistivity: 18.2 MΩ cm), was used to prepare aqueous solutions. Folin-Ciocalteu′s phenol reagent was purchased from Sigma-Aldrich.

2.2. Shrimp waste treatment and extraction procedure

Shrimp processing waste, consisting of the cephalothorax of the red shrimp species *A. foliacea*, was obtained from a local fishing company and stored at −20 °C until use. All samples used in this study were obtained from a single fishing batch collected on February 4th, 2025, from the Ionian Sea (FAO fishing area 37.2.2). The frozen material was homogenized using a blade mill (Retsch Grindomix GM 200) at 10,000 rpm for 10 s and then dried to a constant weight in a fan oven at 50 °C for 5 h. The dried biomass was subsequently ground again under the same conditions to obtain a fine powder. Ethanol and shrimp powder were then mixed at a 5:1 (*v/w, mL/g*) ratio and incubated for 20 min at room temperature under gentle stirring. The mixture was then centrifuged at 5000 g for 5 min, and the resulting supernatant was collected. Solvent removal was carried out using a rotary evaporator (Buki Rotavapor R205), resulting in a thick, reddish-coloured oil, which was referred as crude extract (CE).

2.3. Crude extract fractionation by solvent partitioning

An aliquot of CE (≈ 0.3 g) was first treated with ethyl acetate to solubilize the most hydrophobic components. The ethyl acetate solution was withdrawn and labelled as “hydrophobic fraction” (HF). The pale white material undissolved in ethyl acetate was dried and subsequently redissolved in ethanol, withdrawn, and designated as “polar fraction” (PF). The two fractions were analysed for their mass, AST content, antioxidant capacity and total polyphenolic content.

2.4. AST content assessment

AST concentration in ethanol extracts was evaluated spectrophotometrically using the extinction coefficient of 112 $mM^{-1}cm^{-1}$ at 479 nm. This extinction coefficient was determined based on the known extinction coefficient of AST at 476 nm in acetone (122 mM^{-1} cm^{-1}), by acquiring the visible spectra of equimolar standard solutions of synthetic free AST in ethanol and acetone, following the procedure previously described (Mancarella et al., 2025).

2.5. Antioxidant capacity assessment

The antioxidant activity of CE and its fractions was evaluated using the ABTS decolorization assay following the procedure adopted by Mancarella et al. (Mancarella et al., 2025). All measurements were performed in time course mode using a double beam Varian Cary 2000 spectrophotometer, measuring the absorbance decrease arising from ABTS radical neutralization at 750 nm after 30 min from sample addition. This time interval was necessary due to the slow reaction of carotenoids with ABTS radical (Mastrogiacomo et al., 2015). Since Trolox was used as standard antioxidant compound, the antioxidant activity was expressed as Trolox Equivalent Antioxidant Capacity (TEAC), and the results were presented in micromoles of Trolox equivalents (TE μmol) per gram of sample. All measurements were performed in triplicate.

2.6. Total polyphenolic content assessment

Total phenol content (TPC) was determined following the method described by Magalhães et al. (2010), using a microplate reader (Tecan, Infinite M200). Briefly, 50 μL of Folin-Ciocalteu reagent, previously diluted 1:5 (*v/v*) with Milli-Q water, were dispensed into each well of a 96-well microplate and mixed to 50 μL of sample. Then, 100 μL of sodium hydroxide solution (0.35 M) were added. The absorbance value at 760 nm was recorded after a 5-minute incubation. Gallic acid was employed as the reference standard to obtain a calibration curve within the range 2.5–40.0 mg/L. The TPC of each sample was expressed as micromoles of gallic acid equivalents (GAE μmol) per gram of sample. All measurements were performed in triplicate.

2.7. Fatty acid composition

The fatty acid profile of CE was analysed using the method described by Raju et al. (2021a). Briefly, 0.1 g of CE were dissolved in 1 ml hexane, then trans-esterified with 200 μl of 2 M methanolic sodium hydroxide at 50 °C for 5 min. After cooling, the solution was vortex-mixed, followed by the addition of 200 μL of 2 M methanolic hydrochloric acid. The resulting mixture was thoroughly vortexed and subsequently centrifuged at 3500 g for 10 min at 4 °C. The hexane layer was collected and 1 μL of extract was analysed using gas chromatography coupled to mass spectrometer detector (Agilent GC 8890- MS 5977 A; Santa Clara, CA, USA), with a 5:1 split ratio. The injector temperature was maintained at 250 °C while the column temperature was initially set at 50 °C. This was then programmed to rise at a rate of 20 °C/min up to 200 °C and then elevated to 230 °C at a rate of 3 °C/min. The HP-INNOWAX capillary column (60 m × 0.25 mm × 0.25 μm film) was employed to conduct the separation. Authentic reference standards (Supelco FAME mix, Bellefonte, PA, USA) were used to identify the peaks, and the levels of fatty acids were expressed as relative percentages (Nam et al., 2025). All analyses were conducted in triplicate.

2.8. FTIR spectroscopic measurements

Mid-infrared spectra were acquired using a PerkinElmer Spectrum One FTIR spectrometer equipped with a universal attenuated total reflectance (ATR) apparatus (GladiATR, Pike Technologies). The internal reflection element was a single-bounce diamond microprism with a diameter of 4 mm. The background spectrum was collected with the bare microcrystal, and the sample spectrum was acquired by casting a drop (≈10 μL) of sample onto the diamond surface and allowing the solvent to evaporate. The resolution was set at 4 cm^{-1} and 16 interferograms were acquired and averaged for all spectra.

2.9. Cell treatments and reagents

Human hepatocellular carcinoma cell line HuH7 (cat. #JCRB0403, purchased from JCRB) and human colon cancer cell line HCT15 (cat. #CCL-225, purchased from ATCC) were maintained in low-glucose Dulbecco's Modified Eagle Medium (DMEM, Sigma-Aldrich D5546) supplemented with 10% fetal bovine serum (FBS Capricorn HI-12A), 100 U/mL penicillin, 100 μg/mL streptomycin (Sigma-Aldrich #P4333), and 2 mM glutamine (Sigma-Aldrich G7513). Cells were cultured at 37 °C in a humidified atmosphere with 5% CO_2. Both cell lines were regularly tested for mycoplasma contamination using a Mycoplasma Detection Kit (Aurogene, REP-MYSNC-100). Palmitic acid (PA, Cat. No. 506,345) and fatty acid-free bovine serum albumin (BSA) fraction V (Cat. No. 03,117,057,001) were purchased from Merck. PA was dissolved in BSA at a final molar ratio of approximately 2:1 (fatty acids/BSA), closely resembling the physiological ratio in human serum (Alsabeeh et al., 2018). The solution was diluted at 200 μM concentration in DMEM for cell treatments. CE was dissolved in DMSO to obtain a stock solution at 20 mg/mL concentration, which was subsequently diluted in culture medium to achieve final CE concentrations of 0.1, 0.2, and 0.4 mg/mL, corresponding to final DMSO concentrations of 0.5%, 1%, and 2% (v/v), respectively. Equivalent amounts of DMSO alone were tested in parallel to assess potential solvent toxicity. 20 mg/mL stock solutions in DMSO were prepared also for HF and PF and employed analogously. Cell viability was assessed in adherent cells (at a density of 1×10^4 cells in 96-well plate) using the crystal violet assay, following the protocol described in (Feoktistova et al., 2016); all experimental data were normalized to the viability values obtained from DMSO-treated controls to isolate the specific effects of CE.

The BODIPY stain protocol was used for lipid droplet (LD) analysis. Following fatty acid treatments, cells were seeded onto coverslips in 12-well plates (at a density of 1×10^5 cells/well) at 60–80% confluence. After treatment, cells were washed twice with PBS and incubated for 15 min at 37 °C with BODIPY 493/503 at a dilution of 1:1000 in PBS from a 1 mg/mL stock solution. After that, coverslips were washed three times with PBS and used for rapid image acquisition. Images were captured using a Cell Imaging Station microscope (Invitrogen™, FLoid™ Cell Imaging Station, 10–213–412, ThermoFisher Scientific, Waltham, MA, USA) at 20x magnification with a scale bar of 100 μm. Fluorescence intensity was measured by a Biotek Cytation 5 Cell Imaging Multimode Reader (Agilent Technologies, Santa Clara, CA, USA).

2.10. Oxidative stress and antioxidant activity assay

Reduced glutathione (GSH), hydrogen peroxide (H_2O_2), and malondialdehyde (MDA) levels were measured as indicators of oxidative stress. Hydrogen peroxide was analysed using Amplex™ Red Hydrogen Peroxide/Peroxidase Assay Kit (ThermoFisher #A22188) protocol. Reduced glutathione levels were measured by the sulfhydryl reagent 5,5′-Dithiobis(2-nitrobenzoic acid) (DTNB) as reported by Rahman et al. (2006). MDA levels were measured using the Lipid Peroxidation Assay Kit (Sigma-Aldrich #MAK085). Catalase (CAT) activity was spectrophotometrically measured as reported by Hadwan and Abed (2016). Superoxide Dismutase (SOD) activity was measured using Superoxide Dismutase Activity Assay Kit (Sigma-Aldrich #CS0009). Glutathione Peroxidase (GPx) activity was measured following the instructions reported in the Glutathione Peroxidase Assay Kit (Sigma-Aldrich #MAK437).

2.11. Thin-layer chromatography analysis of lipids

Total lipids were extracted using methyl-tert-butyl ether, following the method described by Matyash et al. (2008). The extracted lipids were subjected to thin-layer chromatography (TLC) by loading them onto silica gel plates. Separation was achieved using a hexane/ethyl ether/acetic acid mixture (70/30/1; *v/v/v*) optimized for neutral lipid fractionation. This system effectively resolves triacylglycerols (TAG), free fatty acids (FFA), cholesterol (CHOL), and diacylglycerols (DAG), while phospholipids (PHOSPHO) are retained at the starting application line. Following the development, the plates were uniformly sprayed with 10% cupric sulphate in 8% aqueous phosphoric acid, dried for 10 min at room temperature, and baked at 145 °C for an additional 10 min, as described by Moliterni et al. (2024). Lipid spot intensities were quantified using the ChemiDoc system (Bio-Rad), with specific lipid species identified through parallel development of corresponding standards under identical conditions.

2.12. Statistical analysis

Data are reported as mean ± standard deviation (SD) or standard error of the mean (SEM). SD was applied to describe the variability among individual observations, while SEM was used when the focus was on the accuracy of the group mean. Statistical differences were evaluated using GraphPad Prism version 8.3.0 for Windows. The comparison was made using a one-way analysis of variance (ANOVA). After Tukey's post hoc analysis, differences between groups were considered statistically significant when $p < 0.05$.

3. Results and discussion

3.1. AST, TPC and TEAC of crude extract

As reported in Table 1, ethanol enabled the extraction of 270 mg of CE per gram of *A. foliacea* cephalothorax powder, while the AST extraction yield was 0.92 μmol/g, corresponding to 537 μg of free pigment per gram of shrimp matrix. This value is extremely interesting since it exceeds typical AST extraction yields reported in the literature for shrimp waste, including the yield of 190 μg/g achieved using abdomen shells of the same shrimp species and eutectic mixtures as extracting solvents (Mancarella et al., 2025). Moreover, our results are in line with extraction yields achieved with the same matrix using ethyl acetate as solvent (670 μg/g) (Milano et al., 2025) and confirm that shrimp cephalothorax is particularly rich in AST pigment, as previously demonstrated by Scurria et al. for *Parapenaeus longirostris* (Scurria et al., 2020). Beyond AST, literature indicates that the cephalothorax is a source of a wide range of bioactive compounds. Specifically, further lipophilic antioxidants, such as tocopherols, are contained in the hepatopancreas, the main reservoir of lipids located into shrimp cephalothorax (Takeungwongtrakul et al., 2012; Gómez-Estaca et al., 2016). On the other side, water extracts from *Litopenaeus vannamei* cephalothorax were found to exhibit antioxidant activity mainly ascribable to peptides (Binsan et al., 2008). More recently, a polyphenol rich fraction obtained from *Pandalus borealis* heads has been described (Onodenalore et al., 2024) and the structures of two unique heterocyclic phenolic compounds have been identified. In the present work the extraction yield of polyphenolic compounds from *A. foliacea* cephalothorax was 7.4 GAE μmol/g, while the overall yield of antioxidant equivalent extraction was 44 TE μmol/g.

Focussing on CE composition, the AST concentration was 3.4 μmol/g, corresponding to 0.2% (*w/w*). Interestingly, the TEAC value (163 TE μmol/g) was higher than that reported by Tsoupras et al. for shrimp oil extracted from the whole biomass (shell and flesh) of *A. foliacea* (15.4 TE μmol/g) using a methanol/chloroform/water solvent mixture (Tsoupras et al., 2025). The observed enhanced antioxidant activity can be thus attributed to the bioactive richness of the cephalothorax matrix combined with the solvent properties of ethanol, which extracts a broader range of antioxidants with diverse polarity.

Table 1
Extraction yields relevant to the crude extract and concentrations of bioactive components in whole and fractionated extracts.

Extraction yields				
Crude extract mass (mg/g) *	*AST (μmol/g)* *	*TEAC (TE μmol/g)* *	*TPC (GAE μmol/g)* *	
270	0.92	44	7.4	
Extract composition				
	mass (g/g) #	*AST (μmol/g)* $	*TEAC (TE μmol/g)* $	*TPC (GAE μmol/g)* $
Crude extract	1	3.4	163	27
Hydrophobic fraction	0.47	6.6	55	not detected
Polar fraction	0.52	0.13	150	29

* Reference mass: dried shrimp heads.
\# Reference mass: crude extract.
$ Reference mass: relevant fraction.

3.2. Fatty acid profile of crude extract

The fatty acid profile of CE, reported in Table 2, highlighted the high content of unsaturated fatty acids, typical of crustaceans. The most abundant fatty acid found in CE was oleic acid (29%), followed by DHA (9.9%), EPA (9.8%) and PA (9.2%). It is well established that shrimp oil composition varies considerably depending on species, anatomical part, environment, and extraction method (Cholidis et al., 2024). Regarding anatomical distribution, previous studies highlighted significant

Table 2
Fatty acid profile of crude extract.

Compound	Number of C atoms and unsaturation	%	±SD
Saturated fatty acids (SFA)			
Lauric acid	C12:0	0.72	0.05
Myristic acid	C14:0	1.63	0.12
Pentadecanoic acid	C15:0	0.64	0.11
Palmitic acid	C16:0	9.22	0.53
Margaric acid	C17:0	0.48	0.24
Stearic acid	C18:0	6.16	0.29
Nonadecanoic acid	C19:0	1.91	0.21
Mono-unsaturated fatty acids (MUFA)			
Palmitoleic acid n-7	C16:1 (n-7)	6.28	0.29
cis-7-methyl-6-hexadecenoic acid	C17:1	1.10	0.21
cis-10-Heptadecenoic acid	C17:1 (n-10)	1.30	0.45
Oleic acid	C18:1 (n-9)	29.50	1.34
Vaccenic acid	C18:1 (n-7)	4.43	0.45
Gadoleic acid	C20:1 (n-9)	1.55	0.28
Gondoic acid	C20:1 (n-9)	1.11	0.15
Erucic acid	C22:1 (n-9)	1.03	0.10
Poly-unsaturated fatty acids (PUFA)			
Linoleic acid	C18:2 (n-6)	2.39	0.62
Linolenic acid	C18:3 (n-6)	0.95	0.18
Stearidonic acid	C18:4 omega 3 (n-3)	0.78	0.23
cis-Eicosadienoic acid	C20:2 (n-6)	2.85	0.61
Arachidonic acid	C20:4 (n-6)	4.54	0.34
Eicosatrienoic acid	C20:3 (n-3)	0.24	0.07
Eicosapentaenoic acid (EPA)	C20:5 omega 3 (n-3)	9.81	0.36
Docosapentaenoic acid (DPA)	C22:5 omega-3 (n-3)	1.48	0.05
Docosahexaenoic acid (DHA)	C 22:6 (n-3)	9.91	0.66
Total			
SFA		**20.76**	**1.55**
MUFA		**46.29**	**3.27**
PUFA		**32.95**	**3.13**

differences between the lipid profiles of cephalothorax and edible muscle (Soultani et al., 2016). Specifically, the lipid profile of the cephalothorax is largely reflective of the hepatopancreas composition, which serves as the primary lipid storage organ in crustaceans, and accumulates significant amounts of energetic mono-unsaturated fatty acids (MUFA). Conversely, muscle tissue tends to incorporate higher levels of PUFA mainly in the form of membrane phospholipids (Soultani et al., 2019; Yu et al., 2020).

Table 3 presents the distribution of fatty acids in lipid extracts obtained from the cephalothorax of *Litopenaeus vannamei, Parapenaeus longirostris, Pandalus borealis* and *Aristaeomorpha foliacea,* as reported in the literature. Mean values have been calculated for L. *vannamei* (n = 6), a tropical species often farmed in coastal estuaries or controlled inland systems, and for the three remaining deep-water species, grouped together (n = 4). Despite wide intrinsic variability (Coefficient of variation (CV) in the range 17–34%), the two groups differ significantly: deep-water species show a marked increase in MUFA (44%vs 24% in L. *vannamei,* p = 0.006) and a lower PUFA content (27%vs 43%, p = 0.03), while saturated fatty acids (SFA) levels remain comparable (~29%). This inversion may be tentatively ascribed to the metabolic adaptation of *P. longirostris, Picoides borealis* and *A. foliacea* to the deep-sea environment, where PUFA are preferentially directed to muscle membranes to maintain fluidity, leaving the hepatopancreas richer in energetic MUFA. In this context, the fatty acid profile of CE, and specifically the high MUFA content (46%), is perfectly consistent with a deep-water shrimp cephalothorax profile.

As can be seen from the data in Table 3, the same research group in two distinct studies (Soultani et al., 2016, 2019) reported considerably different PUFA and SFA levels for *P. longirostris* cephalothorax, despite applying the same extraction procedure. This underscores the influence of additional factors, such as fishing season, diet or specific environment, on the cephalothorax oil composition. The discrepancy observed between the fatty acid profile of our CE and that reported for *A. foliacea* cephalothorax (Soultani et al., 2016) is therefore not surprising. Specifically, while the MUFA levels in our CE are consistent with those found in the previous study (~45%), we observed lower SFA (21%vs 36%) and higher PUFA levels (33%vs 19%). The same trend is observed also considering the mean values for the deep-sea species. Even though the scarcity of available data precludes a solid statistical comparison, the preferential extraction of unsaturated fatty acids by ethanol (Setyawardhani et al., 2024) could potentially account for the low SFA levels observed in our CE. Indeed, Soultani et al. (2016, 2019) obtained their lipid extracts using a different solvent, i.e. a chloroform/methanol/water mixture. Overall, the ability of ethanol to preferentially extract unsaturated fatty acids, as highlighted by our work, combined with its bio-based origin and GRAS classification, renders it a highly attractive solvent for the valorisation of this specific sea-food by-product

Table 3
Fatty acid distribution in lipid extracts from cephalothorax of diverse shrimp species.

Shrimp species	Extraction solvent	SFA (%)	MUFA (%)	PUFA (%)	Ref.
L.*vannamei*	chloroform/methanol/water	29.51	25.91	39.30	Takeungwongtrakul et al. (2012)
L.*vannamei*	n-hexane/isopropanol	38.44	17.24	35.27	Raju et al. (2021b)
L. *vannamei*	n-hexane/isopropanol	14.78	29.68	55.56	Sinthusamran et al. (2018)
L. *vannamei*	ethylacetate	28.90	26.59	44.51	Gómez-Estaca et al. (2016)
L. *vannamei*	ethylacetate	31.34	25.09	43.50	Gómez-Estaca et al. (2017)
L. *vannamei*	n-hexane/isopropanol	30.40	22.25	37.50	Gulzar and Benjakul (2018)
mean±SD		**29±9**	**24±5**	**43±8**	
P. longirostris	chloroform/methanol/water	36.19	43.70	20.11	Soultani et al. (2016)
P. longirostris	chloroform/methanol/water	26.67	35.23	38.10	Soultani et al. (2019)
P. borealis	chloroform/methanol/water	15.67	53.79	30.55	Soultani et al. (2019)
A. foliacea	chloroform/methanol/water	*36.23*	*45.21*	*18.57*	Soultani et al. (2016)
mean±SD		**29 ±10**	**44±8**	**27±9**	

3.3. AST, TPC and TEAC of polar and hydrophobic fractions

As evidenced by data in Table 1, fractionation of the CE by ethyl acetate partitioning resulted in a HF, which contained most of the extracted AST, and a PF, insoluble in ethyl acetate, where polyphenols were selectively collected. TPC in the HF was indeed below the detection limit, while trace amounts of AST were found in the PF. The presence of polyphenols in PF aligns with previous studies on shrimp, which isolated highly polar heterocyclic phenolic compounds and demonstrated their antioxidant activity and potential health benefits (Onodenalore et al., 2024). As reported in Table 1 and depicted in Fig. 1, HF and PF substantially contribute equally to the overall mass of CE. AST recovery after fractionation was very good (92%), leading to a two-fold increase of AST concentration within the HF (6.6 μmol/g). In contrast, only 65% of the CE TEAC was retained across the two fractions and was recovered mainly in the PF. The loss of overall antioxidant activity following fractioning might be influenced by antioxidant synergistic effects within the CE, enhancing its TEAC, and/or by degradation of TPC compounds occurring throughout the CE manipulation. Approximately 55% of the phenolic compounds were indeed either degraded or remained undetected, due to possible limitations of the assay. These results indicate that a significant portion of the overall antioxidant activity resides in the PF, despite its negligible AST content.

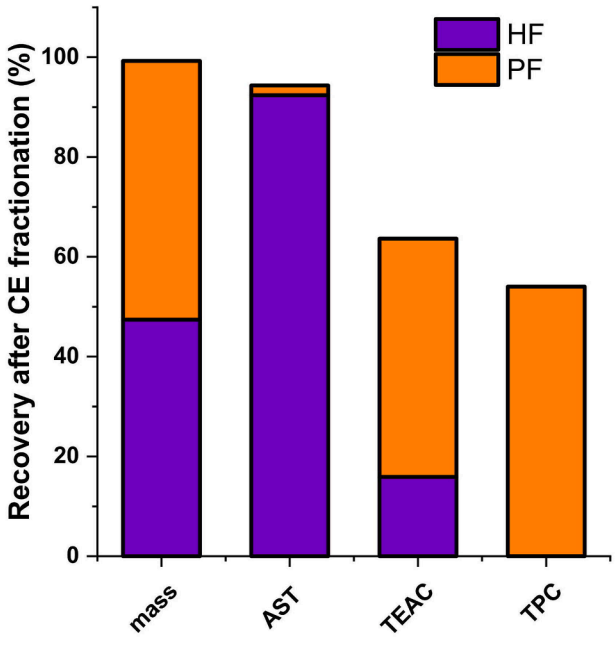

Fig. 1. Mass and bioactives recovery in HF and PF fractions. Recovery yields of mass and bioactive components of crude extract following fractionation into hydrophobic (HF) and polar (PF) fractions. The relative contribution of both fractions is also shown.

3.4. ATR-FTIR analysis

3.4.1. Crude extract

The ATR-FTIR spectra of CE and relevant fractions, reported in Fig. 2, allowed to get information on the bulk components present in these samples. The CE spectrum (black trace) shows sharp and intense bands at 2923 and 2853 cm^{-1}, which can be assigned to methylene group stretching vibrations (Coates, 2006) arising from fatty acid side chains. The peak at 3012 cm^{-1}, due to vinyl C_{sp2}—H stretching, is ascribable to fatty acid unsaturation and agrees with the unsaturation-rich fatty acid profile reported in Table 2. The band at 1461 cm^{-1} can be referred to fatty acid chain too, since arises from methylene bending vibrations. The band at 1740 cm^{-1} is typical of ester compounds (C═O stretching) and highlights the presence of DAG, TAG and PHOSPHO. The broad absorption at 3370 cm^{-1} and the band at 1048 cm^{-1} arise from O—H and C—OH stretching vibrations respectively and can be referred to alcohols. However, the asymmetry of the broad signal with a maximum at 3370 cm^{-1}, indicates diversity in alcohol structures and/or a contribution from amine groups (N—H stretching), as further suggested by the absorption band at 1620 cm^{-1}, which may arise from out-of-plane N—H bending vibrations. Finally, two characteristic peaks at 1582 and 1403 cm^{-1}, likely arising from antisymmetric and symmetric COO^- vibrations respectively, are strongly indicative of the presence of carboxylate groups (Giotta et al., 2011) in the CE.

3.4.2. Hydrophobic fraction

After fractionation into HF and PF, functional groups proved to distribute differently into the two samples. Specifically, HF spectrum (red trace in Fig. 2) presents a major contribution from fatty acid chain absorptions. The carbonyl stretching band, showing a maximum at 1741 cm^{-1}, exhibits a shoulder at 1720 cm^{-1}, suggesting the presence of free fatty acids together with fatty acid esters. This hypothesis is supported by the broad absorption at 3310 cm^{-1} arising from O—H stretching vibration. This absorption band likely presents a contribution from alcoholic O—H vibrations too, as suggested by the C—OH stretching signal at 1055 cm^{-1}. Alcohol marker bands are not surprising in HF, since the presence of sterols, including CHOL, are expected. The characteristic band of CHOL at 1377 cm^{-1} (methyl bending vibration) further outlines the presence of this hydrophobic compound in HF.

3.4.3. Polar fraction

The spectrum of PF (blue trace in Fig. 2) presents much less intense signals ascribable to fatty acid chains, while the absorptions assigned to carboxylate (1584 and 1403 cm^{-1}), amine (1620 cm^{-1}) and alcoholic hydroxyl groups (3374 and 1047 cm^{-1}) are well evident and characteristic of this fraction. The signal at 1515 cm^{-1} and multiple overlapped bands in the region 1650–1500 cm^{-1} suggests the presence of aromatic rings.

To support infrared band assignment and safely recognize main components of PF, the sensitivity of absorption signals to treatment with strong acids was assessed. To this aim 0.1 mL of HCl 0.1 N were added to 1.5 mg of PF and the mixture was vortexed for 30 min. A 3 µL aliquot of the resulting slurry was layered onto the ATR crystal and the FTIR spectrum was acquired after solvent evaporation. Interestingly the

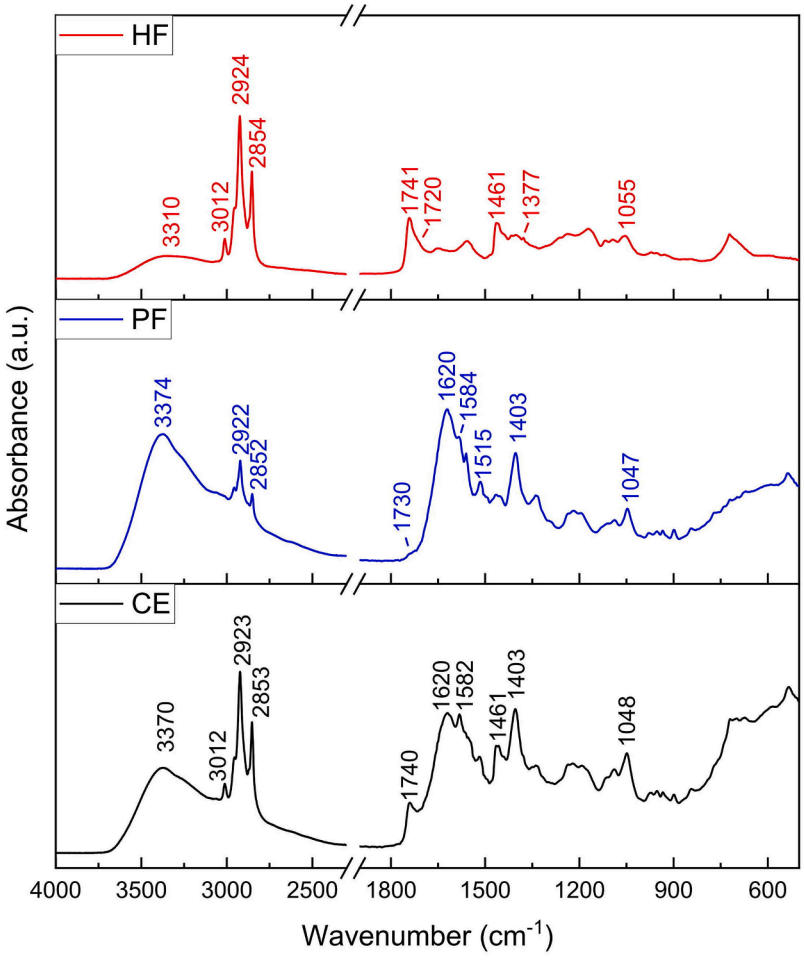

Fig. 2. ATR-FTIR profiles of crude extract and fractions. ATR-FTIR spectra of crude extract (CE, black trace) and of polar (PF, blue trace) and hydrophobic (HF, red trace) fractions.

spectrum of HCl-treated PF, shown in the Supplementary Material (Figure S1), lacks the signals at 1584 and 1403 cm^{-1} attributed to carboxylate groups, while new signals at 1732 and 1215 cm^{-1} appear, in agreement with COO^- protonation and consequent formation of free carboxylic acids (Giotta et al., 2011). Moreover, the simultaneous appearing of broad absorptions in the 3100–2600 cm^{-1} region suggests the protonation of primary amine groups.

Overall, the infrared spectroscopic analysis indicated that main components of the PF are PHOSPHO with polar heads bearing alcoholic (inositol, glycerol), amine (ethanolamine) or aminoacidic (serine) groups, polyphenol compounds (hydroxyl and aromatic ring moieties) and fatty acid salts (methylene and carboxylate groups). However, it is not excluded the presence of further classes of compounds such as free aminoacids and/or free sugars rich in hydroxyl and carboxylate moieties.

3.5. Cell viability and lipid droplet accumulation in hepatic and intestinal cells

To evaluate the impact of CE on cell viability, intestinal (HCT15) and hepatic (HuH7) cell lines were treated with three different concentrations of the extract. While 0.1 mg/mL and 0.2 mg/mL showed no significant effects on cell viability at 12, 24, or 48 h, exposure to 0.4 mg/mL for 48 h resulted in marked cytotoxicity in both cell types, indicating that prolonged exposure to higher concentrations of CE may compromise cell survival (Fig. 3A, B). These results were corroborated by microscopic observations, which revealed evident morphological alterations in cells exposed to increasing concentrations of CE (see Supplementary Material, Figure S2). No appreciable morphological changes were detected in either HCT15 or HuH7 cells exposed to 0.1 and 0.2 mg/mL of CE for 48 h, with cells retaining a regular shape and confluence comparable to controls. By contrast, treatment of cells with 0.4 mg/mL for 48 h induced clear signs of cytotoxicity, including pronounced cellular shrinkage, rounding, detachment from the culture surface and reduced density, consistent with loss of viability. All experimental data were normalized to the viability values obtained from DMSO-treated controls to isolate the specific effects of CE. Morphological representations of the cells exposed to DMSO, as well as the corresponding viability data, are provided in the Supplementary Material (Figure S3). At 0.1 and 0.2 mg/mL of CE, the concentration of DMSO, used as solvent, (0.5% *v/v* and 1% *v/v*, respectively), did not affect cell viability or morphology, whereas at 0.4 mg/mL of CE the concentration of DMSO (2% *v/v*) induced a modest reduction in cell viability at 48 h, affecting both cell lines, particularly HCT15 cells, accompanied by evident morphological alterations, including cell rounding and detachment (Supplementary Material, Figure S3). Based on these findings, the concentration of 0.2 mg/mL for 24 h was selected as the optimal condition for subsequent experiments.

Chemical analysis of the CE revealed abundance of unsaturated fatty acids, which can be readily esterified into TAG, providing an ideal substrate for intracellular lipid droplet (LD) synthesis. Consistent with this composition, treatment of hepatic (HuH7) and intestinal (HCT15) cells with the CE induced a dose-dependent accumulation of LDs, as shown by BODIPY staining, following treatment with 0.1 mg/mL and 0.2 mg/mL of CE (Figs. 3C, D). This effect was reproduced primarily by HF, rich in FFA, TAG, DAG, and CHOL, whereas PF, lacking neutral lipids, did not stimulate LD formation. Notably, CE exhibited an oleic-to-PA ratio of approximately 3:1. In a previous study, we demonstrated that co-treatment with oleic acid and PA at a 1:1 ratio reduced PA-induced lipotoxicity compared with PA alone, supporting a protective role of oleic acid mediated by LD formation (Moliterni et al., 2024). Consistent with this evidence, CE may contribute to the sequestration of potentially toxic fatty acids into triacylglycerols (TAGs), a metabolically safe storage form, thereby mitigating lipotoxic stress.

3.6. Crude extract rescues palmitic acid-induced toxicity in hepatic and intestinal cells

Saturated fatty acids, particularly PA, are well-documented inducers of lipotoxicity in various cell types, including hepatic and intestinal cells (Moliterni et al., 2024). PA has been shown to trigger cell dysfunction and reduced viability (Listenberger et al., 2003; Wei et al., 2006). These mechanisms make PA a widely used experimental model to investigate lipotoxic damage and evaluate the efficacy of potential protective agents.

To evaluate the protective potential of CE against PA-induced lipotoxicity, hepatic HuH7 and intestinal HCT15 cells were treated with PA alone or in combination with CE. As expected, PA exposure resulted in a marked reduction in cell viability in both cell lines (Fig. 4A and B). Interestingly, co-treatment with CE significantly mitigated the cytotoxic effects of PA, as evidenced by higher cell viability (Fig. 4A and B). Microscopic analysis further supported these findings, showing fewer structural abnormalities in cells treated with both PA and CE compared to those treated with PA alone. Specifically, PA exposure caused

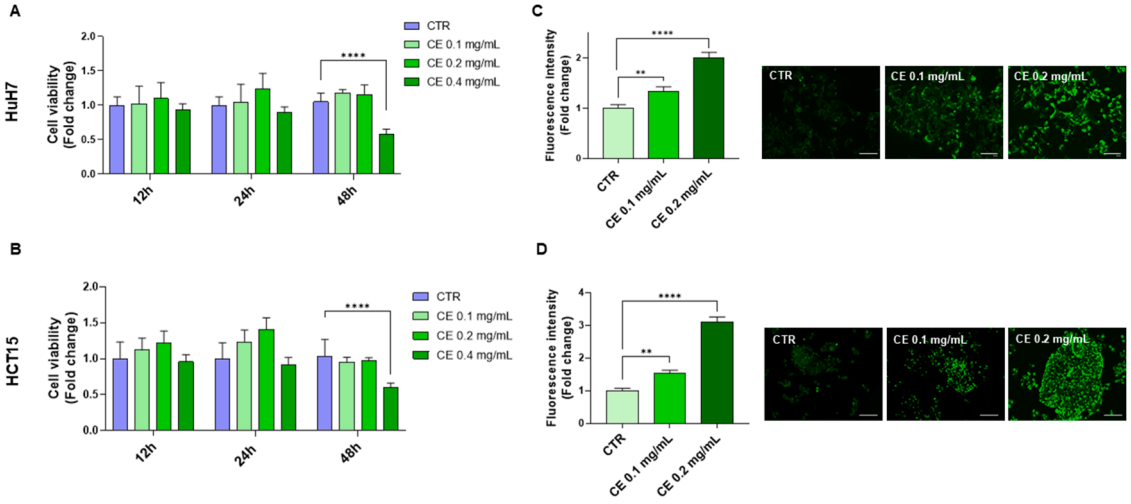

Fig. 3. Effect of CE on cell viability and lipid accumulation. (A, B) Cell viability assay performed on HuH7 and HCT15 cells treated for 12, 24, and 48 h with crude extract (CE) at concentrations of 0.1, 0.2, and 0.4 mg/mL. **(C, D)** Representative fluorescence microscopy images of HuH7 and HCT15 cells stained with BODIPY 493/503 to visualize lipid droplets (LDs) after treatment with CE and relative quantification of BODIPY fluorescence intensity in HuH7 and HCT15 cells. Scale bars = 100 μm. Data are expressed as mean ± *SE (n = 3). CTR: untreated control. (**) p < 0.01; (****) p < 0.001.*

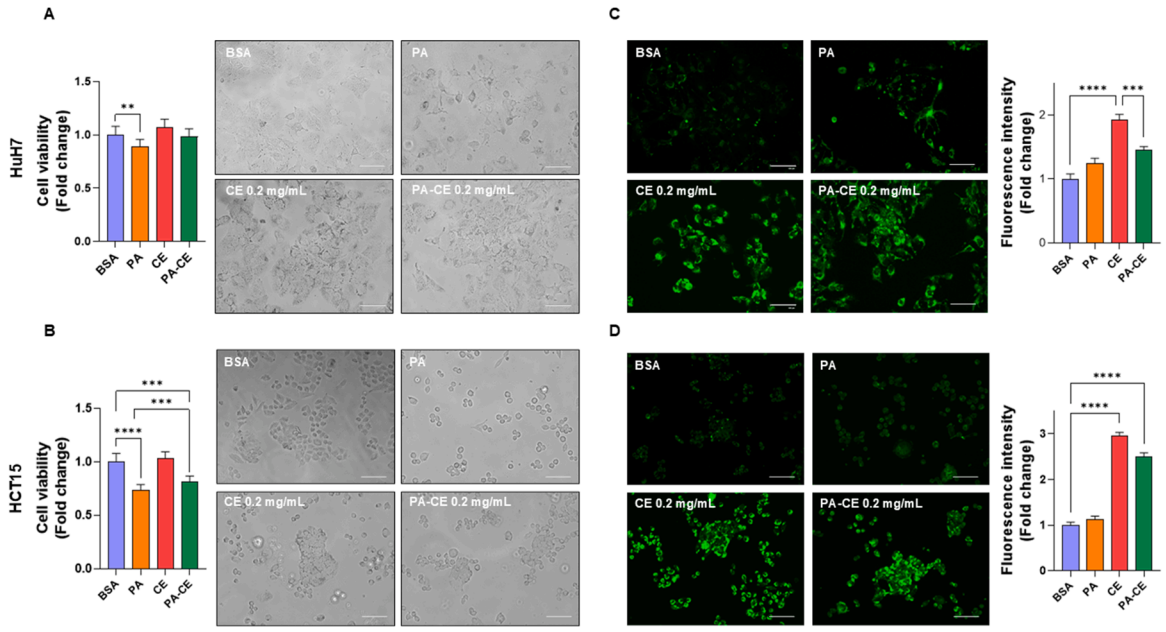

Fig. 4. Effects of CE on PA-induced lipotoxicity. (A, B) Cell viability of HuH7 and HCT15 cells treated for 24 h with BSA (bovine serum albumin, vehicle control), palmitic acid (PA), crude extract (CE) (0.2 mg/mL), or the combination PA-CE, assessed by crystal violet assay, and respective phase-contrast microscopy images of HuH7 (A) and HCT15 (B) cells after the same treatments. **(C, D)** Representative fluorescence microscopy images of BODIPY 493/503 staining, and corresponding quantification of BODIPY fluorescence intensity in HuH7 and HCT15 cells. Scale bars = 100 μm. Data represent the means ± SE of three independent experiments. (*) $p < 0.05$; (**) $p < 0.01$; (***) $p < 0.005$; (****) $p < 0.001$.

pronounced morphological alterations, including cell rounding, detachment, and a marked reduction in cell density. In contrast, co-treatment with CE largely preserved normal cell structure, restoring morphology to conditions closely resembling controls and thereby markedly reducing PA-induced cytotoxic damage. In HuH7 cells, PA treatment led to LD accumulation, which was further enhanced by co-treatment with CE, as evidenced by fluorescence imaging, which revealed a marked increase in fluorescence intensity (Fig. 4C). Conversely, in HCT15 cells, PA induced a little LD accumulation that was increased by co-treatment with the extract, also supported by fluorescence observations compared to the control (Fig. 4D). Thus, CE demonstrated strong cytoprotective activity against PA-induced lipotoxicity, a condition characterized by oxidative stress, membrane lipid peroxidation, and depletion of endogenous antioxidant defences.

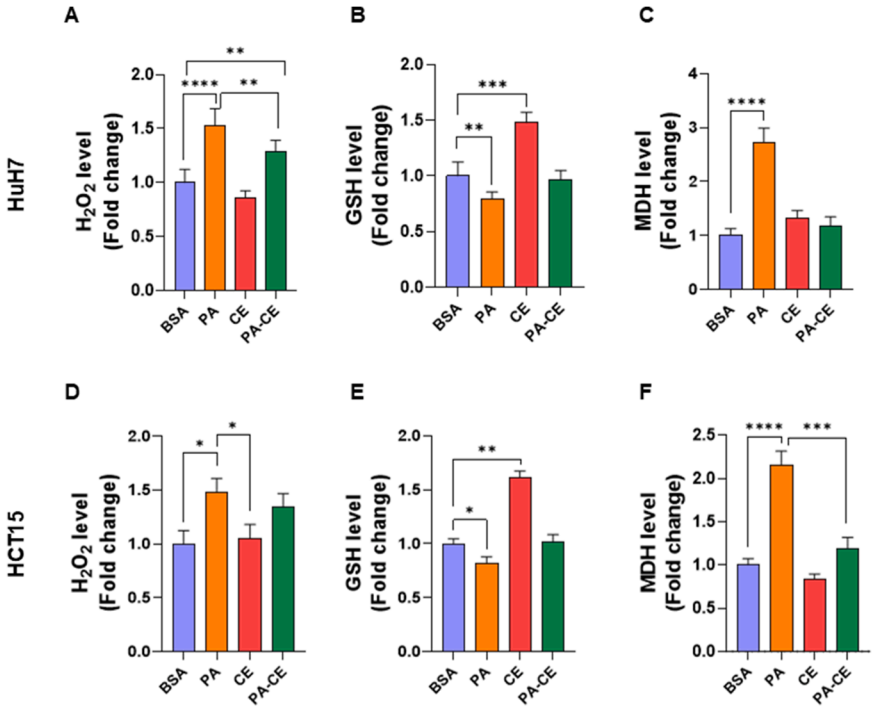

Fig. 5. Effects of CE on oxidative stress markers. Panels (**A**), (**B**), and (**C**) show the H_2O_2, GSH, and MDA levels, respectively, in HuH7 cells. Panels (**D**), (**E**), and (**F**) represent the H_2O_2, GSH, and MDA levels, respectively, in HCT15 cells. Both cell lines were treated for 24 h with BSA, palmitic acid (PA) 200 μM, crude extract (CE) (0.2 mg/mL), or the combination PA-CE. Data are expressed as mean ± SE of three different measures. (*) $p < 0.05$, (**) $p < 0.01$, (***) $p < 0.005$, (****) $p < 0.001$.

3.7. Crude extract modulates oxidative stress in palmitic acid-treated hepatic and intestinal cells

To investigate the protective effects of CE against PA-induced toxicity, we assessed key oxidative stress markers in HuH7 and HCT15 cells. Specifically, we measured levels of H_2O_2, GSH, and MDA following PA treatment, both in the presence and absence of CE. These markers were chosen due to their well-established roles in cellular redox homeostasis and as indicators of oxidative damage (Katerji et al., 2019), providing a comprehensive view of the antioxidant ability of CE. H_2O_2, a major by-product of oxidative metabolism, functions as an important mediator of cellular signalling at physiological concentrations, playing roles in cell proliferation, differentiation, and apoptosis (Di Marzo et al., 2018; Sies, 2017). However, an excessive accumulation of H_2O_2 is widely recognized as a significant contributor to oxidative stress, leading to the oxidation of lipids and proteins, and DNA damage (Njie-Mbye et al., 2013; Schieber & Chandel, 2014). Consistent with previous research demonstrating PA's pro-oxidative effects (Moliterni et al., 2024), our results showed that PA treatment led to a marked increase in H_2O_2 levels in both HuH7 and HCT15 cell lines (Fig. 5A, D). This aligns with the understanding that saturated fatty acids like PA can overload mitochondrial respiration, leading to increased ROS production, including H_2O_2 (Listenberger et al., 2003). Crucially, CE addition significantly reduced H_2O_2 accumulation in both cell lines, further supporting its established role in mitigating oxidative stress by modulating mitochondrial function and ROS generation (Afzal et al., 2023).

GSH is a crucial intracellular antioxidant, fundamental in neutralizing ROS and maintaining cellular redox balance (Jiao et al., 2023). As the most abundant endogenous antioxidant, GSH directly scavenges free radicals and acts as a substrate for various antioxidant enzymes, such as GPx. Consequently, a reduction in GSH levels is commonly associated with increased oxidative stress and cellular damage, compromising the cell's ability to detoxify harmful oxidants (Ballatori et al., 2009; Sekhar et al., 2011). In our experiments, PA exposure significantly decreased GSH levels in both hepatic (HuH7) and intestinal (HCT15) cell lines, indicating a substantial burden of oxidative stress and depletion of the cellular antioxidant capacity. This finding is consistent with literature showing that PA-induced lipotoxicity often depletes GSH reserves (Alnahdi et al., 2019). However, co-treatment with CE effectively restored GSH levels in both HuH7 and HCT15 cells (Fig. 5B, E). This suggests that CE either directly enhances GSH synthesis, preserves existing GSH by reducing ROS load, or upregulates enzymes involved in GSH regeneration, thereby bolstering the cellular antioxidant defence system.

MDA is a widely recognized and frequently used biomarker of lipid peroxidation, a process in which ROS damage cellular membranes by oxidizing polyunsaturated fatty acids (Ayala et al., 2014; Del Rio et al., 2005). Elevated MDA levels are a direct indicator of increased oxidative stress and severe cellular membrane damage (Ayala et al., 2014; Cordiano et al., 2023). In our study, PA treatment resulted in a significant rise in MDA levels in both hepatic HuH7 and intestinal HCT15 cell lines (Fig. 5C and F), unequivocally confirming the induction of lipid peroxidation and membrane integrity compromise. This observation aligns with the known mechanisms of PA-induced lipotoxicity, where excessive fatty acids lead to mitochondrial dysfunction and subsequent oxidative assault on cellular membranes (Sies, 2017). Notably, co-treatment with CE effectively lowered MDA levels in both cell lines (Fig. 5C and F), demonstrating its potent ability to counteract PA-induced oxidative damage and preserve membrane integrity. This protective effect of CE against lipid peroxidation further underscores its broad antioxidant properties, potentially by reducing the initial ROS generation or by enhancing cellular antioxidant defences that mitigate lipid damage.

These collective findings strongly suggest that CE protects against PA-induced cytotoxicity in hepatic and intestinal cells through a multifaceted mechanism involving a significant reduction in overall oxidative stress, the preservation of crucial intracellular antioxidant defences, and the prevention of deleterious lipid peroxidation. This comprehensive protective action highlights CE's potential as a therapeutic agent in conditions characterized by oxidative stress and lipotoxicity.

3.8. Crude extract modulates antioxidant enzyme activity

To further elucidate the protective mechanisms of CE against PA-induced toxicity, we investigated the activity of critical endogenous antioxidant enzymes, namely catalase, GPx, and SOD-1. These enzymes represent essential components of the cell's defence system against ROS and were analysed in hepatic HuH7 and intestinal HCT15 cells following PA treatment, both in the presence and absence of CE. Catalase is a ubiquitous antioxidant enzyme that plays a crucial role in the detoxification of H_2O_2, thereby preventing the accumulation of this oxidant (Anwar et al., 2024). A reduction in catalase expression or activity is indicative of impaired cellular defence against oxidative stress and can exacerbate oxidative damage (Choi et al., 2009; Pizzino et al., 2017). Our analysis revealed that PA exposure significantly reduced catalase enzymatic activity in both HuH7 and HCT15 cell lines, suggesting a compromised ability to neutralize H_2O_2 and an overall weakened antioxidant defence. This finding aligns with previous studies indicating that lipotoxicity can impair antioxidant enzyme systems (Hauck & Bernlohr, 2016). Crucially, co-treatment with CE effectively restored catalase activity in HuH7 (Fig. 6A) and HCT15 (Fig. 6D) cells. This suggests that CE actively supports the cellular antioxidant machinery, potentially by directly influencing gene expression or by preserving enzyme stability, thereby boosting the cell's capacity to detoxify harmful peroxides.

SOD constitutes the first line of defence against oxidative stress by catalysing the dismutation of superoxide radicals ($O_2^{\cdot-}$) into oxygen and H_2O_2, thereby preventing the formation of more harmful ROS species (Fridovich, 1995). Specifically, SOD is a cytosolic enzyme crucial for maintaining redox balance within the cytoplasm. A significant decrease in SOD activity, as we observed following PA exposure, indicates an overwhelming burden of superoxide radicals and a compromised ability to neutralize ROS (Tacconi et al., 2023; Zheng et al., 2023). However, co-treatment with CE effectively restored SOD activity in both HuH7 and HCT15 cells (Fig. 6B, E), further supporting its broad protective role against oxidative stress. To note that CE alone was able to significantly increase SOD activity in hepatic HuH7 cells (Fig. 6B). The restoration of SOD activity is paramount, as it directly reduces the initial burst of superoxide, thereby mitigating the downstream cascade of oxidative damage.

GPx is a key selenoenzyme in the cellular antioxidant defence, catalysing the reduction of hydrogen peroxide and lipid hydroperoxides to water and corresponding alcohols by oxidizing GSH, thereby preventing oxidative damage to lipids, proteins, and DNA (Zhao et al., 2018). A decrease in GPx levels or activity directly correlates with increased lipid peroxidation and subsequent oxidative damage, making cells more vulnerable to cytotoxic insults (Alnahdi et al., 2019; Lubos et al., 2011). In HuH7 and HCT15 cells, GPx activity was measured at 24 h of treatment with PA, CE, or their combination. Our results demonstrated that PA treatment significantly downregulated GPx activity in both cell lines, indicating a heightened susceptibility to lipid damage and a diminished capacity to manage oxidative stress. This is consistent with PA's known role in inducing lipotoxicity and membrane dysfunction (Alnahdi et al., 2019). In contrast, CE treatment increased GPx activity, indicating upregulation of the selenoenzyme system by bioactive shrimp-derived compounds (Pei, Pan, Wei & Hua, 2023). Notably, the co-administration of CE effectively prevented this PA-induced reduction in GPx (Fig. 6C and F), thereby preserving cellular antioxidant capacity. This protective effect highlights CE's potential to counteract lipid peroxidation, which is a hallmark of PA-induced cellular injury.

The coexistence of LD-promoting and antioxidant activities in the ethanol extract may be mechanistically linked: LDs can sequester

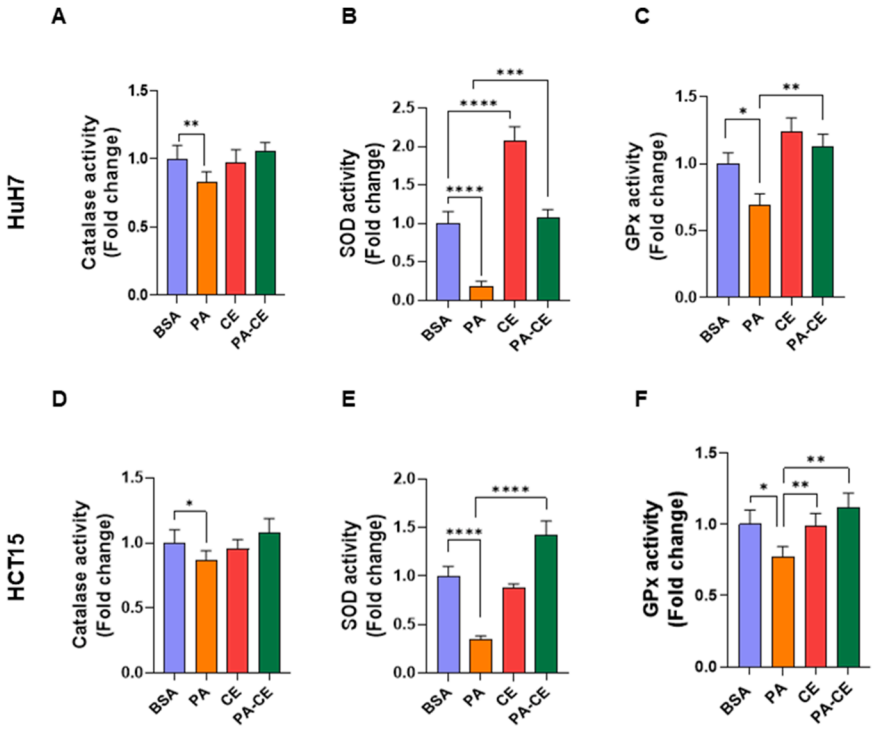

Fig. 6. Effects of CE on antioxidant enzyme activity in HuH7 and HCT15 cells. (**A**), (**B**), and (**C**) Catalase, superoxide dismutase (SOD) and glutathione peroxidase (GPx) activity in HuH7 and (**D**), (**E**) and (**F**) HCT15 cells. Cells were treated with BSA (control), palmitic acid (PA) (200 μM), crude extract (CE) (0.2 mg/mL), or PA-CE. Data are presented as fold change relative to control (BSA). Statistical significance: (*) $p < 0.05$, (**) $p < 0.01$, (***) $p < 0.001$, (****) $p < 0.0001$.

oxidizable PUFAs away from membranes, thereby reducing the substrate pool for lipid peroxidation, while antioxidant enzymes and

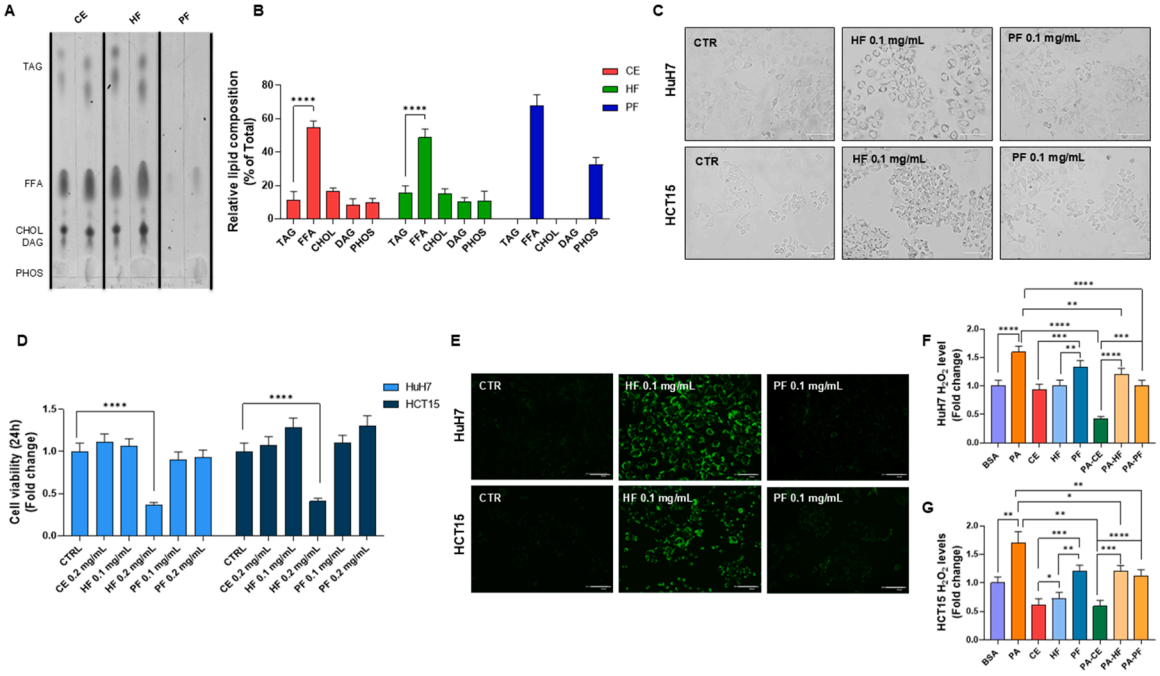

Fig. 7. Characterization of CE fractions and their effects on cell lipid composition and viability. (**A**) Representative TLC bands of major lipid classes of the crude extract (CE) extract and its hydrophobic (HF) and polar (PF) components: triacylglycerols (TAG), free fatty acids (FFA), cholesterol (CHOL), diacylglycerols (DAG), and phospholipids (PHOSPHO). (**B**) Relative abundance (% of total lipids) of each lipid class in CE, HF, and PF, quantified by densitometry. (**C**) Phase-contrast microscopy images of HuH7 and HCT15 cells treated for 24 h with CE (0.2 mg/mL), HF (0.1 mg/mL), and PF (0.1 mg/mL), compared to untreated controls (CTR). (**D**) Cell viability of HuH7 and HCT15 cells treated for 24 h with CE (0.2 mg/mL), HF, and PF at both 0.1 mg/mL and 0.2 mg/mL, assessed by crystal violet assay. (**E**) Representative fluorescence microscopy images of BODIPY staining in HuH7 and HCT15 cells treated with HF or PF (0.1 mg/mL). Scale bars = 100 μm. (**F**) H_2O_2 level in HuH7 and (**G**) HCT15 cells. Both cell lines were treated for 24 h with BSA, palmitic acid (PA) 200 μM, crude extract (CE) (0.2 mg/mL), HF (0.1 mg/mL), PF (0.1 mg/mL), or a combination of PA-HF and PA-PF. Data are the means of three different analyses. (*) $p < 0.05$; (**) $p < 0.01$; (***) $p < 0.005$; (****) $p < 0.001$.

compounds limit ROS-mediated LD degradation and the release of toxic lipid intermediates (Listenberger et al., 2003; Olzmann & Carvalho, 2019). In this way, the high unsaturated fatty acid content of *A. foliacea* cephalothorax extract not only drives LD biogenesis but, in concert with its diverse antioxidant components, contributes to a dual protective strategy, physically isolating excess fatty acids in a safe storage form and chemically neutralizing oxidative threats. This coordinated action supports cellular redox homeostasis, preserves membrane integrity, and mitigates lipotoxic stress, highlighting the extract's potential as a nutraceutical or pharmaceutical ingredient for the prevention or management of oxidative stress-related disorders.

3.9. Polar and hydrophobic fractions of CE reduce palmitic acid-induced lipotoxicity

To better understand the contribution of the distinct components of the CE extract to its biological activity and LD accumulation, we analysed the lipid composition of the HF and PF fractions by TLC. This analysis enabled us to determine the distribution of the major neutral lipid classes within each fraction compared to the whole extract. We then evaluated the individual effects of HF and PF to assess their potential cytoprotective properties and ability to promote LD accumulation.

In agreement with FTIR analysis, the CE extract was primarily composed of FFA (54.6%), along with lower levels of TAG (11.3%), CHOL (16.5%), DAG (8.2%), and PHOSPHO (9.4%) (Fig. 7A and B). All these lipid classes were also present in the HF fraction, maintaining similar relative proportions. Coherent with the FTIR spectrum, the PF fraction contained only FFA and PHOSPHO (Fig. 7A and B).

To assess cytotoxicity, HuH7 and HCT15 cells were treated for 24 h with CE (0.2 mg/mL), as well as with HF and PF at two concentrations, 0.1 mg/mL (matching their estimated content in the total extract) and 0.2 mg/mL. At 0.1 mg/mL, neither HF nor PF induced cytotoxic effects, as confirmed by both phase-contrast microscopy (Fig. 7C) and viability assays (Fig. 7D). The phase-contrast images show that cell morphology and confluency remain comparable to untreated control cells (CTR), indicating that HF and PF are not cytotoxic at this concentration. However, treatment with HF, and not PF, at 0.2 mg/mL resulted in a marked reduction in cell viability in both cell lines, suggesting that the cytotoxic effect of CE is attributable to the HF fraction. Additionally, representative morphological images of both cell lines treated with 0.2 mg/mL HF and 0.2 mg/mL PF further support the quantitative findings (see Supplementary Material, Fig.e S4).

BODIPY staining revealed that only HF, and not PF, was capable of inducing LD accumulation in HuH7 and HCT15 cells when used at 0.1 mg/mL (Fig. 7E). These data agree with the major presence of FFA in the HF fraction.

Moreover, we assayed the antioxidant potential of the two different components of CE. Thus, intracellular H_2O_2 levels in HuH7 and HCT15 cells were quantified following 24 h of treatment with BSA (vehicle control), PA, CE, HF, PF, and each combination with PA at their respective working concentrations. As expected, PA alone induced a significant increase in H_2O_2 in both HuH7 and HCT15 lines. Treatment with CE, HF, and PF alone reduced basal H_2O_2 levels in both cell lines (Fig. 7F and G). Co-treatment of PA with total extract markedly attenuated the PA-induced rise in H_2O_2 (Fig. 7F and G). Co-treatment of PA with either of the two isolated fractions (HF and PF) reduces its pro-oxidant effect, although to a lesser extent than the combined fractions in the whole ethanol extract (CE) (Fig. 7F and G). Notably, HF and PF alone exerted a partial attenuation of PA-induced oxidative stress (PA vs. PA-HF and PA-PF). In contrast, the combined fraction (CE) in the presence of PA (PA-CE) produced the strongest reduction in H_2O_2 levels, restoring values well below those observed with PA alone, and also significantly different from PA-HF and PA-PF (Figs. 7F and G). This finding indicates that the concomitant presence of hydrophobic and polar bioactive compounds in CE confers a superior protective effect, supporting a synergistic interaction between HF and PF fractions. Together, these findings indicate that the high unsaturated fatty acid content of CE underlies its capacity to promote LD formation, a process that may contribute to its overall protective effect by safely storing excess fatty acids and reducing lipotoxic damage. At the same time, the synergistic antioxidant action of its lipid and non-lipid components helps maintain redox homeostasis, preserve membrane integrity, and support endogenous antioxidant defences, making the ethanol extract of *A. foliacea* cephalothorax a promising candidate for nutraceutical or pharmaceutical applications targeting oxidative stress-related conditions.

The remarkably high FFA content of CE (54.6%) is indicative of extensive post-mortem lipolysis, likely driven by the phospholipases and lipases abundantly present in the hepatopancreas, which represents the main lipid storage and digestive organ in the shrimp cephalothorax. The liberation of PUFAs from their esterified forms renders them susceptible to oxidative degradation, with potential generation of pro-oxidant species such as lipid hydroperoxides and secondary aldehydes. However, given the strong net antioxidant capacity exhibited by CE both in chemical assays (TEAC: 163 TE μmol/g) and in cell-based experiments, it can be concluded that any pro-oxidant contribution is substantially outweighed by the overall protective activity of the extract.

4. Conclusions

This study demonstrates that ethanol extraction is an effective and sustainable strategy for the valorisation of *Aristaeomorpha foliacea* cephalothorax, a distinct bioactive-rich by-product of the fishing industry.

The resulting CE exhibited a valuable chemical profile, characterized by high yields of AST and polyphenols, alongside a fatty acid composition remarkably rich in MUFA and PUFA. Specifically, the exceptionally high MUFA content (46%) appears to be a characteristic trait of the cephalothorax in deep-sea shrimp species, as evidenced by statistical analysis of literature data. The low level of SFA is equally noteworthy, warranting further investigation into the role of ethanol selectivity in this finding. The fractionation process revealed that while AST and neutral lipids are concentrated in the hydrophobic fraction, the polar fraction retains a significant portion of the antioxidant power, which can be ascribed only partially to the presence of polar phenolic compounds, highlighting the chemical complexity of the matrix.

From a biological perspective, the CE displayed potent cytoprotective effects in hepatic and intestinal cell lines challenged with PA-induced lipotoxicity. Our findings suggest that this protection relies on a dual mechanism of action. First, the high content of unsaturated fatty acids in the extract promotes the biogenesis of LDs, facilitating the safe sequestration of excess free fatty acids into neutral triacylglycerols, thereby mitigating membrane stress. Second, the extract exerts a strong antioxidant activity by scavenging intracellular ROS (H_2O_2), preventing lipid peroxidation (MDA reduction), and restoring the pool of endogenous antioxidant defences (GSH, Catalase, SOD, and GPx) depleted by PA treatment. Notably, the comparative analysis of the isolated fractions indicates a synergistic effect within the CE. While the hydrophobic fraction drives the adaptive lipid storage response and the polar fraction contributes significantly to radical scavenging, the whole extract offers superior protection against oxidative stress compared to either fraction alone.

Collectively, these results support the potential of *A. foliacea* cephalothorax ethanol extract as a cost-effective and high-value nutraceutical ingredient capable of targeting metabolic and oxidative stress-related disorders, thus promoting a circular economy approach in the seafood sector. In this context, future investigations should focus on verifying ethanol's preferential extraction of unsaturated fatty acids and bioactives subsequently elucidating the underlying mechanisms. A deeper understanding of this selectivity could guide the optimization of sustainable extraction protocols, aiming to produce lipid preparations

with enriched unsaturation profiles, specific antioxidant pools and maximized health-promoting value. Furthermore, the therapeutic value of the shrimp oil described in this study appears extremely promising, particularly considering that its biological activity may be further enhanced by addressing the lipolytic degradation of the raw matrix due to cephalothorax enzymes. Minimizing this predictable aspect, by reducing the time between catch and extraction, is expected to yield preparations with a lower pro-oxidant burden and an even more potent antioxidant and cytoprotective profile, further strengthening the applicative potential of this seafood by-product as a functional ingredient.

Declaration of generative AI and AI-assisted technologies in the writing process

During the preparation of this work the authors used Chat-GPT in order to improve language and readability of the manuscript. After using this tool, the authors reviewed and edited the content as needed and take full responsibility for the content of the publication.

Ethical statement – studies in humans and animals

The authors declare that the research presented did not involve any animal or human study.

CRediT authorship contribution statement

Ilaria Serra: Data curation, Formal analysis, Investigation, Visualization, Validation, Writing – original draft, Writing – review & editing. **Federica Mancarella:** Data curation, Investigation, Validation, Visualization, Writing – review & editing. **Paola Semeraro:** Data curation, Investigation, Methodology, Writing – review & editing. **Maria Tufariello:** Investigation, Methodology, Validation, Visualization, Writing – review & editing. **Alessandro Miraglia:** Investigation, Validation, Visualization, Writing – review & editing. **Marcello Chieppa:** Conceptualization, Validation, Supervision, Writing – review & editing. **Aurelia Scarano:** Investigation, Validation, Visualization, Writing – review & editing. **Angelo Santino:** Formal analysis, Supervision, Funding acquisition, Writing – review & editing. **Daniele Vergara:** Formal analysis, Resources, Writing – review & editing. **Elisa Bisconti:** Investigation, Visualization, Writing – review & editing. **Francesco Vari:** Investigation, Visualization, Writing – review & editing. **Ludovico Valli:** Formal analysis, Supervision, Funding acquisition, Writing – review & editing. **Livia Giotta:** Conceptualization, Formal analysis, Data curation, Methodology, Supervision, Validation, Visualization, Writing – original draft, Writing – review & editing. **Anna Maria Giudetti:** Conceptualization, Data curation, Formal analysis, Methodology, Supervision, Validation, Visualization, Writing – original draft, Writing – review & editing. **Francesco Milano:** Conceptualization, Data curation, Formal analysis, Methodology, Supervision, Validation, Visualization, Writing – original draft.

Declaration of competing interest

The authors declare that they have no known competing financial interests or personal relationships that could have appeared to influence the work reported in this paper.

Reports a relationship with that includes:. Has patent pending to. If there are other authors, they declare that they have no known competing financial interests or personal relationships that could have appeared to influence the work reported in this paper.

Acknowledgements

This work was funded by the European Union through "PON Ricerca e Innovazione 2014–2020″ of the Italian Ministry for Universities and Research (MUR), Action IV.4 and IV.6 and under the National Recovery and Resilience Plan (PNRR), Mission 4 Component 2 Investment 1.3, Theme 10 "ON Foods—Research and Innovation Network on Food and Nutrition Sustainability, Safety, and Security—Working ON Foods". The project: "IDENTITA - rete Integrata meDiterranea per l'osservazione ed Elaborazione di percorsi di Nutrizione personalizzaTa contro la malnuTrizione"- T5-AN-01 (PUGLIA REGION - Health Marketplace Coordination) is also acknowledged.

The authors are grateful to Orazio Albano (Aquaculture and Sustainable Blue Food consultant) and Gabriella Chieffo (Entropya srl) for their support in this project and to Prof. Tiziano Verri for helpful discussions.

Supplementary materials

Supplementary material associated with this article can be found, in the online version, at doi:10.1016/j.afres.2026.102325.

Data availability

Data will be made available on request.

References

Afzal, S., Abdul Manap, A. S., Attiq, A., Albokhadaim, I., Kandeel, M., & Alhojaily, S. M. (2023). From imbalance to impairment: The central role of reactive oxygen species in oxidative stress-induced disorders and therapeutic exploration. *Frontiers in Pharmacology, 14*, Article 1269581. https://doi.org/10.3389/fphar.2023.1269581

Alnahdi, A., John, A., & Raza, H. (2019). N-acetyl cysteine attenuates oxidative stress and glutathione-dependent redox imbalance caused by high glucose/high palmitic acid treatment in pancreatic Rin-5F cells. *PLOS ONE, 14*(12), Article e0226696. https://doi.org/10.1371/journal.pone.0226696

Alsabeeh, N., Chausse, B., Kakimoto, P. A., Kowaltowski, A. J., & Shirihai, O. (2018). Cell culture models of fatty acid overload: Problems and solutions. *Biochimica et Biophysica Acta (BBA) – Molecular and Cell Biology of Lipids, 1863*(2), 143–151. https://doi.org/10.1016/j.bbalip.2017.11.006

Aneesh, P. A., Anandan, R., Kumar, L. R. G., Ajeeshkumar, K. K., Kumar, K. A., & Mathew, S. (2023). A step to shell biorefinery—Extraction of astaxanthin-rich oil, protein, chitin, and chitosan from shrimp processing waste. *Biomass Conversion and Biorefinery, 13*(1), 205–214. https://doi.org/10.1007/s13399-020-01074-5

Anwar, S., Alrumaihi, F., Sarwar, T., Babiker, A. Y., Khan, A. A., Prabhu, S. V., & Rahmani, A. H. (2024). Exploring therapeutic potential of Catalase: Strategies in disease prevention and management. *Biomolecules, 14*(6), 697. https://www.mdpi.com/2218-273X/14/6/697.

Ayala, A., Muñoz, M. F., & Argüelles, S. (2014). Lipid peroxidation: Production, metabolism, and signaling mechanisms of malondialdehyde and 4-hydroxy-2-nonenal. *Oxidative Medicine and Cellular Longevity, 2014*(1), 1–31. https://doi.org/10.1155/2014/360438

Ballatori, N., Krance, S. M., Notenboom, S., Shi, S., Tieu, K., & Hammond, C. L. (2009). Glutathione dysregulation and the etiology and progression of human diseases. *Biological Chemistry, 390*(3), 191–214. https://doi.org/10.1515/BC.2009.033

Battino, M., Giampieri, F., Cianciosi, D., Ansary, J., Chen, X., Zhang, D., … Forbes-Hernández, T. (2021). The roles of strawberry and honey phytochemicals on human health: A possible clue on the molecular mechanisms involved in the prevention of oxidative stress and inflammation. *Phytomedicine : International Journal of Phytotherapy and Phytopharmacology, 86*, Article 153170. https://doi.org/10.1016/j.phymed.2020.153170

Binsan, W., Benjakul, S., Visessanguan, W., Roytrakul, S., Tanaka, M., & Kishimura, H. (2008). Antioxidative activity of Mungoong, an extract paste, from the cephalothorax of white shrimp (Litopenaeus vannamei). *Food Chemistry, 106*, 185–193. https://doi.org/10.1016/j.foodchem.2007.05.065

Bohn, T. (2019). Carotenoids and markers of oxidative stress in Human observational studies and intervention trials: Implications for chronic diseases. *Antioxidants, 8*(6), 179. https://doi.org/10.3390/antiox8060179

Bungau, S., Abdel-Daim, M. M., Tit, D. M., Ghanem, E., Sato, S., Maruyama-Inoue, M., … Kadonosono, K. (2019). Health benefits of polyphenols and carotenoids in age-related eye diseases. *Oxidative Medicine and Cellular Longevity, 2019*(1), 1–22. https://doi.org/10.1155/2019/9783429

Cheong, J. Y., Muskhazli, M., Nor Azwady, A. A., Ahmad, S. A., & Adli, A. A. (2020). Three dimensional optimisation for the enhancement of astaxanthin recovery from shrimp shell wastes by Aeromonas hydrophila. *Biocatalysis and Agricultural Biotechnology, 27*, Article 101649. https://doi.org/10.1016/j.bcab.2020.101649

Choi, S.-I., Kim, T.-I., Kim, K. S., Kim, B.-Y., Ahn, S.-Y., Cho, H.-J., … Kim, E. K. (2009). Decreased catalase expression and increased susceptibility to oxidative stress in primary cultured corneal fibroblasts from patients with granular corneal dystrophy type II. *The American Journal of Pathology, 175*(1), 248–261. https://doi.org/10.2353/ajpath.2009.081001

Cholidis, P., Kranas, D., Chira, A., Galouni, E. A., Adamantidi, T., Anastasiadou, C., & Tsoupras, A. (2024). Shrimp lipid bioactives with anti-inflammatory,

antithrombotic, and antioxidant health-promoting properties for cardio-protection. *Marine Drugs, 22*, 554. https://doi.org/10.3390/md22120554
Coates, J. (2006). Interpretation of infrared spectra, A practical approach. In *Encyclopedia of analytical chemistry*.
Cordiano, R., Di Gioacchino, M., Mangifesta, R., Panzera, C., Gangemi, S., & Minciullo, P. L. (2023). Malondialdehyde as a potential oxidative stress marker for allergy-oriented diseases: An update. *Molecules (Basel, Switzerland), 28*(16), 5979. https://doi.org/10.3390/molecules28165979
Del Rio, D., Stewart, A. J., & Pellegrini, N. (2005). A review of recent studies on malondialdehyde as toxic molecule and biological marker of oxidative stress. *Nutrition, Metabolism and Cardiovascular Diseases, 15*(4), 316–328. https://doi.org/10.1016/j.numecd.2005.05.003
Deng, J.-J., Mao, H.-H., Fang, W., Li, Z.-Q., Shi, D., Li, Z.-W., … Luo, X.-C. (2020). Enzymatic conversion and recovery of protein, chitin, and astaxanthin from shrimp shell waste. *Journal of Cleaner Production, 271*, Article 122655. https://doi.org/10.1016/j.jclepro.2020.122655
Di Marzo, N., Chisci, E., & Giovannoni, R. (2018). The role of hydrogen peroxide in redox-dependent signaling: Homeostatic and pathological responses in mammalian cells. *Cells, 7*(10), 156. https://doi.org/10.3390/cells7100156
Djuricic, I., & Calder, P. C. (2021). Beneficial outcomes of omega-6 and omega-3 polyunsaturated fatty acids on Human health: An update for 2021. *Nutrients, 13*(7), 2421. https://doi.org/10.3390/nu13072421
Donia, T., & Khamis, A. (2021). Management of oxidative stress and inflammation in cardiovascular diseases: Mechanisms and challenges. *Environmental Science and Pollution Research, 28*(26), 34121–34153. https://doi.org/10.1007/s11356-021-14109-9
Dua, K., Malyla, V., Singhvi, G., Wadhwa, R., Krishna, R. V., Shukla, S. D., … Hansbro, P. M. (2019). Increasing complexity and interactions of oxidative stress in chronic respiratory diseases: An emerging need for novel drug delivery systems. *Chemico-Biological Interactions, 299*, 168–178. https://doi.org/10.1016/j.cbi.2018.12.009
Feoktistova, M., Geserick, P., & Leverkus, M. (2016). Crystal violet assay for determining viability of cultured cells. *Cold Spring Harbor protocols, 2016*(4), Article pdb.prot087379. https://doi.org/10.1101/pdb.prot087379. pdb.prot087379.
Fotodimas, I., Ioannou, Z., & Kanlis, G. (2024). A review of the benefits of the sustainable utilization of shrimp waste to produce novel foods and the impact on Human health. *Sustainability, 16*(16), 6909. https://doi.org/10.3390/su16166909
Fridovich, I. (1995). Superoxide radical and superoxide dismutases. *Annual Review of Biochemistry, 64*, 97–112. https://doi.org/10.1146/annurev.bi.64.070195.000525
Gammone, M.A., Riccioni, G., & D'Orazio, N. (2015). Carotenoids: Potential allies of cardiovascular health? *Food & Nutrition Research,* 26762. https://doi.org/10.3402/fnr.v59.26762.
Giotta, L., Mastrogiacomo, D., Italiano, F., Milano, F., Agostiano, A., Nagy, K., … Trotta, M. (2011). Reversible binding of metal ions onto bacterial layers revealed by protonation-induced ATR-FTIR difference spectroscopy. *Langmuir :The ACS Journal of Surfaces and Colloids, 27*(7), 3762–3773. https://doi.org/10.1021/la104868m
Gómez-Estaca, J., Montero, P., Fernandez-Martin, F., Calvo, M. M., & Gómez-Guillén, M. C. (2016). The effect of high-pressure treatment on functional components of shrimp (Litopenaeus vannamei) cephalothorax. *Innovative Food Science & Emerging Technologies, 34*, 154–160. https://doi.org/10.1016/j.ifset.2016.01.017
Gómez-Estaca, J., Calvo, M. M., Álvarez-Acero, I., Montero, P., & Gómez-Guillén, M. C. (2017). Characterization and storage stability of astaxanthin esters, fatty acid profile and α-tocopherol of lipid extract from shrimp (L. vannamei) waste with potential applications as food ingredient. *Food Chemistry, 216*, 37–44. https://doi.org/10.1016/j.foodchem.2016.08.016
Gulzar, S., & Benjakul, S. (2018). Ultrasound waves increase the yield and carotenoid content of lipid extracted from cephalothorax of Pacific White shrimp (Litopenaeus vannamei). *European Journal of Lipid Science and Technology, 120*, Article 1700495. https://doi.org/10.1002/ejlt.201700495
Hadwan, M. H., & Abed, H. N. (2016). Data supporting the spectrophotometric method for the estimation of catalase activity. *Data in Brief, 6*, 194–199. https://doi.org/10.1016/j.dib.2015.12.012
Hauck, A. K., & Bernlohr, D. A. (2016). Oxidative stress and lipotoxicity. *Journal of Lipid Research, 57*(11), 1976–1986. https://doi.org/10.1194/jlr.R066597
Hussain, T., Tan, B., Yin, Y., Blachier, F., Tossou, M. C. B., & Rahu, N. (2016). Oxidative stress and inflammation: What polyphenols can do for us? *Oxidative Medicine and Cellular Longevity, 2016*, Article 7432797. https://doi.org/10.1155/2016/7432797
Jiao, Y.-T., Kang, Y.-R., Wen, M.-Y., Wu, H.-Q., Zhang, X.-W., & Huang, W.-H. (2023). Fast antioxidation kinetics of glutathione intracellularly monitored by a dual-wire nanosensor. *Angewandte Chemie International Edition, 62*(51), Article e202313612. https://doi.org/10.1002/anie.202313612
Katerji, M., Filippova, M., & Duerksen-Hughes, P. (2019). Approaches and methods to measure oxidative stress in clinical samples: Research applications in the cancer field. *Oxidative Medicine and Cellular Longevity, 2019*(1), 1–29. https://doi.org/10.1155/2019/1279250
Kaulmann, A., & Bohn, T. (2014). Carotenoids, inflammation, and oxidative stress—Implications of cellular signaling pathways and relation to chronic disease prevention. *Nutrition Research, 34*(11), 907–929. https://doi.org/10.1016/j.nutres.2014.07.010
Kaya, A., Ural, G. N., & Topuz, O. K. (2025). Optimization of ultrasonication-assisted astaxanthin extraction conditions from red giant shrimp (Aristaeomorpha foliacea) processing waste. *Journal of Aquatic Food Product Technology, 34*, 82–91. https://doi.org/10.1080/10498850.2025.2483208
Li, S., Hong, M., Tan, H.-Y., Wang, N., & Feng, Y. (2016). Insights into the role and interdependence of oxidative stress and inflammation in liver diseases. *Oxidative Medicine and Cellular Longevity, 2016*(1), Article 4234061. https://doi.org/10.1155/2016/4234061
Listenberger, L. L., Han, X., Lewis, S. E., Cases, S., Farese, R. V., Ory, D. S., & Schaffer, J. E. (2003). Triglyceride accumulation protects against fatty acid-induced lipotoxicity. *Proceedings of the National Academy of Sciences, 100*(6), 3077–3082. https://doi.org/10.1073/pnas.0630588100
Lubos, E., Loscalzo, J., & Handy, D. E. (2011). Glutathione peroxidase-1 in health and disease: From molecular mechanisms to therapeutic opportunities. *Antioxid Redox Signal, 15*(7), 1957–1997. https://doi.org/10.1089/ars.2010.3586
Magalhães, P. J., Vieira, J. S., Gonçalves, L. M., Pacheco, J. G., Guido, L. F., & Barros, A. A. (2010). Isolation of phenolic compounds from hop extracts using polyvinylpolypyrrolidone: Characterization by high-performance liquid chromatography–diode array detection–electrospray tandem mass spectrometry. *Journal of Chromatography A, 1217*(19), 3258–3268. https://doi.org/10.1016/j.chroma.2009.10.068
Mancarella, F., Milano, F., Semeraro, P., Leo, V. D., Messa, F., Perrone, S., … Valli, L. (2025). Binary mixtures of menthol and alkanoic acids as green solvents for efficient astaxanthin recovery from aristaeomorpha foliacea shrimp shells. *Separation and Purification Technology, 371*, Article 133261. https://doi.org/10.1016/j.seppur.2025.133261
Mastrogiacomo, D., Lenucci, M. S., Bonfrate, V., Di Carolo, M., Piro, G., Valli, L., … Giotta, L. (2015). Lipid/detergent mixed micelles as a tool for transferring antioxidant power from hydrophobic natural extracts into bio-deliverable liposome carriers: The case of lycopene rich oleoresins. *RSC Advances, 5*(4), 3081–3093. https://doi.org/10.1039/C4RA12254B
Matyash, V., Liebisch, G., Kurzchalia, T. V., Shevchenko, A., & Schwudke, D. (2008). Lipid extraction by methyl-tert-butyl ether for high-throughput lipidomics. *Journal of Lipid Research, 49*(5), 1137–1146. https://doi.org/10.1194/jlr.D700041-JLR200
Milano, F., Mancarella, F., Giotta, L., Citro, I., Trocino, S., Calogero, G., & Spadaro, D. (2025). Fast and green process to obtain astaxanthin-rich extracts from shrimp shell waste for dye sensitized solar cells. *Process Biochemistry, 156*, 308–316. https://doi.org/10.1016/j.procbio.2025.06.006
Moliterni, C., Vari, F., Schifano, E., Tacconi, S., Stanca, E., Friuli, M., … Giudetti, A. M. (2024). Lipotoxicity of palmitic acid is associated with DGAT1 downregulation and abolished by PPARα activation in liver cells. *Journal of Lipid Research, 65*(12), Article 100692. https://doi.org/10.1016/j.jlr.2024.100692
Moura, F. A., de Andrade, K. Q., dos Santos, J. C. F., Araújo, O. R. P., & Goulart, M. O. F. (2015). Antioxidant therapy for treatment of inflammatory bowel disease: Does it work? *Redox Biology, 6*, 617–639. https://doi.org/10.1016/j.redox.2015.10.006
Nam, J.-K., Kwak, B.-M., & Jang, H. W. (2025). Optimization and comparative analysis of quality characteristics and volatile profiles in edible insect oils extracted using supercritical fluid extraction and ultrasound-assisted extraction methods. *Food Chemistry, 474*, Article 143237. https://doi.org/10.1016/j.foodchem.2025.143237
Njie-Mbye, Y. F., Chitnis, M. K., Opere, C. A., & Ohia, S. E. (2013). Lipid peroxidation: Pathophysiological and pharmacological implications in the eye. *Frontiers in Physiology, 4*, 366. https://doi.org/10.3389/fphys.2013.00366
Olzmann, J. A., & Carvalho, P. (2019). Dynamics and functions of lipid droplets. *Nature Reviews Molecular Cell Biology, 20*(3), 137–155. https://doi.org/10.1038/s41580-018-0085-z
Onodenalore, A. C., Hossain, A., Banoub, J., & Shahidi, F. (2024). Unique heterocyclic phenolic compounds from shrimp (Pandalus borealis) and beyond. *Food Production, Processing and Nutrition, 6*(1), 29. https://doi.org/10.1186/s43014-023-00215-3
Oppedisano, F., Macrì, R., Gliozzi, M., Musolino, V., Carresi, C., Maiuolo, J., … Mollace, V. (2020). The anti-inflammatory and antioxidant properties of n-3 PUFAs: Their role in cardiovascular protection. *Biomedicines, 8*(9), 306. https://www.mdpi.com/2227-9059/8/9/306.
Pei, J., Pan, X., Wei, G., & Hua, Y. (2023). Research progress of glutathione peroxidase family (GPX) in redoxidation. *Frontiers in Pharmacology, 14*, Article 1147414. https://doi.org/10.3389/fphar.2023.1147414
Peña-Oyarzun, D., Bravo-Sagua, R., Diaz-Vega, A., Aleman, L., Chiong, M., Garcia, L., … Lavandero, S. (2018). Autophagy and oxidative stress in non-communicable diseases: A matter of the inflammatory state? *Free Radical Biology and Medicine, 124*, 61–78. https://doi.org/10.1016/j.freeradbiomed.2018.05.084
Pizzino, G., Irrera, N., Cucinotta, M., Pallio, G., Mannino, F., Arcoraci, V., … Bitto, A. (2017). Oxidative stress: Harms and benefits for Human health. *Oxidative Medicine and Cellular Longevity, 2017*, Article 8416763. https://doi.org/10.1155/2017/8416763
Rahman, I., Kode, A., & Biswas, S. K. (2006). Assay for quantitative determination of glutathione and glutathione disulfide levels using enzymatic recycling method. *Nature Protocols, 1*(6), 3159–3165. https://doi.org/10.1038/nprot.2006.378
Raju, N., Singh, A., & Benjakul, S. (2021a). Recovery, reusability and stability studies of beta cyclodextrin used for cholesterol removal from shrimp lipid. *RSC Advances, 11*(37), 23113–23121. https://doi.org/10.1039/D1RA03282H
Raju, N., Gulzar, S., Buamard, N., Ma, L., Ying, X., Zhang, B., & Benjakul, S. (2021b). Comparative study of astaxanthin, cholesterol, fatty acid profiles, and quality indices between shrimp oil extracted from hepatopancreas and cephalothorax. *Frontiers in Nutrition, 8*, Article 803664. https://doi.org/10.3389/fnut.2021.803664
Roy, V. C., Getachew, A. T., Cho, Y.-J., Park, J. S., & Chun, B. S. (2020). Recovery and bio-potentialities of astaxanthin-rich oil from shrimp (Penaeus monodon) waste and mackerel (Scomberomous niphonius) skin using concurrent supercritical CO2 extraction. *The Journal of Supercritical Fluids, 159*, Article 104773. https://doi.org/10.1016/j.supflu.2020.104773
Sánchez-Camargo, A. P., Martinez-Correa, H. A., Paviani, L. C., & Cabral, F. A. (2011). Supercritical CO2 extraction of lipids and astaxanthin from Brazilian redspotted shrimp waste (Farfantepenaeus paulensis). *The Journal of Supercritical Fluids, 56*(2), 164–173. https://doi.org/10.1016/j.supflu.2010.12.009

Saw, C. L. L., Yang, A. Y., Guo, Y., & Kong, A.-N. T. (2013). Astaxanthin and omega-3 fatty acids individually and in combination protect against oxidative stress via the Nrf2–ARE pathway. *Food and Chemical Toxicology, 62*, 869–875. https://doi.org/10.1016/j.fct.2013.10.023

Schieber, M., & Chandel, N. S. (2014). ROS function in redox signaling and oxidative stress. *Current Biology, 24*(10), R453–R462. https://doi.org/10.1016/j.cub.2014.03.034

Scurria, A., Fabiano Tixier, A.-S., Lino, C., Pagliaro, M., D'Agostino, F., Avellone, G., & Ciriminna, R. (2020). High yields of shrimp oil rich in omega-3 and natural astaxanthin from shrimp waste. *ACS Omega, 5*(28), 17500–17505. https://doi.org/10.1021/acsomega.0c01978

Sekhar, R. V., Patel, S. G., Guthikonda, A. P., Reid, M., Balasubramanyam, A., Taffet, G. E., & Jahoor, F. (2011). Deficient synthesis of glutathione underlies oxidative stress in aging and can be corrected by dietary cysteine and glycine supplementation1234. *The American Journal of Clinical Nutrition, 94*(3), 847–853. https://doi.org/10.3945/ajcn.110.003483

Setyawardhani, D. A., Majid, D. A., & Plawi, R. S. S. (2024). Solid-liquid equilibrium study of binary system saturated fatty acid in short chain alcohols. *Equilibrium Journal of Chemical Engineering, 8*(1), 8. https://doi.org/10.20961/equilibrium.v8i1.80577

Seyedsadjadi, N., & Grant, R. (2021). The potential benefit of monitoring oxidative stress and inflammation in the prevention of non-communicable diseases (NCDs). *Antioxidants, 10*(1), 15. https://doi.org/10.3390/antiox10010015

Sharayei, P., Azarpazhooh, E., Zomorodi, S., Einafshar, S., & Ramaswamy, H. S. (2021). Optimization of ultrasonic-assisted extraction of astaxanthin from green tiger (Penaeus semisulcatus) shrimp shell. *Ultrasonics Sonochemistry, 76*, Article 105666. https://doi.org/10.1016/j.ultsonch.2021.105666

Sies, H. (2017). Hydrogen peroxide as a central redox signaling molecule in physiological oxidative stress: Oxidative eustress. *Redox Biology, 11*, 613–619. https://doi.org/10.1016/j.redox.2016.12.035

Sinthusamran, S., Benjakul, S., Kijroongrojana, K., Prodpran, T., & Agustini, T. W. (2018). Yield and chemical composition of lipids extracted from solid residues of protein hydrolysis of Pacific white shrimp cephalothorax using ultrasound-assisted extraction. *Food Bioscience, 26*, 169–176. https://doi.org/10.1016/j.fbio.2018.10.009

Soultani, G., Strati, I. F., Zoumpoulakis, P., Miniadis-Meimaroglou, S., & Sinanoglou, V. J. (2016). Assessment of functional lipid constituents of red (*Aristaeomorpha foliacea*) and pink (*Parapenaeus longirostris*) shrimps. *Journal of Aquaculture Research and Development, 07*(10), 452. https://doi.org/10.4172/2155-9546.1000452

Soultani, G., Sinanoglou, V. J., Stathopoulou, E., Rasmussen, R. R., Jacobsen, C., Komaitis, M., & Sloth, J. J. (2019). Evaluation of lead, mercury, cadmium and arsenic accumulation, and fatty acids'profile in muscle and cephalothorax of *Parapenaeus longirostris* (Mediterranean shrimp) and of *Pandalus borealis* (northern shrimp). *International Food Research Journal, 26*, 175–185.

Tacconi, S., Longo, S., Guerra, F., Moliteni, C., Friuli, M., Romano, A., Gaetani, S., Paradiso, V. M., Difonzo, G., Caponio, F., Lofrumento, D., Vergara, D., Bucci, C., Dini, L., & Giudetti, A. M. (2023). An aqueous olive leaf extract (OLE) ameliorates parameters of oxidative stress associated with lipid accumulation and induces lipophagy in human hepatic cells. *Food & Function, 14*(12), 5805–5819. https://doi.org/10.1039/D3FO00817G

Takeungwongtrakul, S., Benjakul, S., & H-kittikun, A. (2012). Lipids from cephalothorax and hepatopancreas of Pacific white shrimp (Litopenaeus vannamei): Compositions and deterioration as affected by iced storage. *Food Chemistry, 134*, 2066–2074. https://doi.org/10.1016/j.foodchem.2012.04.003

Tsoupras, A., Cholidis, P., Kranas, D., Galouni, E. A., Ofrydopoulou, A., Efthymiopoulos, P., Shiels, K., Kumar Saha, S., Kyzas, G. Z., & Anastasiadou, C. (2025). Anti-inflammatory, antithrombotic, and antioxidant properties of amphiphilic lipid bioactives from shrimp. *Pharmaceuticals, 18*(1), 25. https://doi.org/10.3390/ph18010025

Wang, J.-L., Yu, Z.-L., Yin, F.-W., Li, D.-Y., Liu, H.-L., Song, L., & Zhou, D.-Y. (2021). Comparison of different solvents for extraction of oils from by-products of shrimps Penaeus vannamei and Procambarus clarkia. *Journal of Food Processing and Preservation, 45*, Article e15754. https://doi.org/10.1111/jfpp.15754

Wei, Y., Wang, D., Topczewski, F., & Pagliassotti, M. J. (2006). Saturated fatty acids induce endoplasmic reticulum stress and apoptosis independently of ceramide in liver cells. *American Journal of Physiology-Endocrinology and Metabolism, 291*(2), E275–E281. https://doi.org/10.1152/ajpendo.00644.2005

Yu, Z., Li, D., Yin, F., Zhao, Q., Liu, Z., Song, L., Zhou, D., & Wang, T. (2020). Lipid profiles in by-products and muscles of three shrimp species (Penaeus monodon, Penaeus vannamei, and Penaeus chinensis). *European Journal of Lipid Science and Technology, 122*, Article 1900309. https://doi.org/10.1002/ejlt.201900309

Zhao, L., Zong, W., Zhang, H., & Liu, R. (2019). Kidney toxicity and response of selenium containing protein-glutathione peroxidase (Gpx3) to CdTe QDs on different levels. *Toxicological Sciences, 168*(1), 201–208. https://doi.org/10.1093/toxsci/kfy297

Zhazykbayeva, S., Pabel, S., Mügge, A., Sossalla, S., & Hamdani, N. (2020). The molecular mechanisms associated with the physiological responses to inflammation and oxidative stress in cardiovascular diseases. *Biophysical Reviews, 12*(4), 947–968. https://doi.org/10.1007/s12551-020-00742-0

Zheng, M., Liu, Y., Zhang, G., Yang, Z., Xu, W., & Chen, Q. (2023). The applications and mechanisms of superoxide dismutase in medicine, food, and cosmetics. *Antioxidants, 12*(9), 1675. https://doi.org/10.3390/antiox12091675

Zuluaga, M., Barzegari, A., Letourneur, D., Gueguen, V., & Pavon-Djavid, G. (2017). Oxidative stress regulation on endothelial cells by hydrophilic astaxanthin complex: Chemical, biological, and molecular antioxidant activity evaluation. *Oxidative Medicine and Cellular Longevity, 2017*(1), Article 8073798. https://doi.org/10.1155/2017/8073798

Further reading

Sriket, P., Benjakul, S., Visessanguan, W., & Kijroongrojana, K. (2007). Comparative studies on chemical composition and thermal properties of black tiger shrimp (Penaeus monodon) and white shrimp (Penaeus vannamei) meats. *Food Chemistry, 103*, 1199–1207. https://doi.org/10.1016/j.foodchem.2006.10.039

Yerlikaya, P., Topuz, O. K., Buyukbenli, H. A., & Gokoglu, N. (2013). Fatty acid profiles of different shrimp species: Effects of depth of catching. *Journal of Aquatic Food Product Technology, 22*(3), 290–297. https://doi.org/10.1080/10498850.2011.646388

Glossary

ABTS: 2,2′-azinobis(3-ethylbenzothiazoline-6-sulfonate)
AST: Astaxanthin
ATR: Attenuated total reflectance
BSA: Bovine serum albumin
CAT: Catalase
CE: Crude extract
CHOL: Cholesterol
CTR: Untreated control
DAG: Diacylglycerols
DHA: Docosahexaenoic acid
DMEM: Dulbecco's Modified Eagle Medium
DMSO: Dimethyl sulfoxide
DPA: Docosapentaenoic acid
DTNB: 5,5′-Dithiobis(2-nitrobenzoic acid)
EPA: Eicosapentaenoic acid
FBS: Fetal bovine serum
FFA: Free fatty acids
GAE: Gallic acid equivalents
GPx: Glutathione Peroxidase
GSH: Reduced glutathione
H_2O_2: Hydrogen peroxide
HCT15: Human intestinal cell line
HF: Hydrophobic fraction
HuH7: Human hepatic cell line
LD: Lipid droplet
MDA: Malondialdehyde
MUFA: Monounsaturated fatty acids
NCDs: Non-communicable diseases
PA: Palmitic acid
PF: Polar fraction
PHOSPHO: Phospholipids
PUFA: Polyunsaturated fatty acids
ROS: Reactive oxygen species
SD: Standard deviation
SFA: Saturated fatty acids
SOD: Superoxide dismutase
TAG: Triacylglycerols
TEAC: Trolox Equivalent Antioxidant Capacity
TE: Trolox equivalents
TLC: Thin-layer chromatography
TPC: Total phenolic content